Slurry Reactors for Gas-to-Liquid Processes: A Review

Tiefeng Wang,* Jinfu Wang, and Yong Jin

Beijing Key Laboratory of Green Reaction Engineering and Technology, Department of Chemical Engineering, Tsinghua University, Beijing 100084, China

With the dramatic increase in the international oil price, gas-to-liquid processes of Fischer−Tropsch (FT) synthesis, methanol synthesis, and dimethyl ether (DME) synthesis have become increasingly important and received much attention from both academic and industrial interests. The slurry reactor has the advantages of simple construction, excellent heat transfer performance, online catalyst addition and withdrawal, and a reasonable interphase mass transfer rate with low energy input, which make it very suitable for gas-to-liquid processes. However, its multiphase flow behaviors are very complex and the multiphase reactor has some remarkable scale-up effects; therefore, extensive studies are still needed for the development and design of a high-performance slurry reactor. This article gives a state-of-the-art review of the recent studies on the slurry reactor for gas-to-liquid processes. The influences of the superficial gas velocity, operating pressure and temperature, solid concentration, column dimensions, and gas distributor are discussed. Some recent developments in the liquid−solid separation in a slurry reactor are also summarized. The concept of using internals to intensify the mass transfer and improve the hydrodynamics is discussed based on both experimental results and theoretical analysis. Modeling and simulations of the gas−liquid and gas−liquid−solid flows are briefly reviewed, with focus on the new trend of coupling the population balance model (PBM) into the computational fluid dynamics (CFD) framework to describe the complex bubble behaviors and gas−liquid interphase interactions. The results of a 3000 ton/year pilot plant for DME synthesis are given, showing that the slurry reactor has promising applications in gas-to-liquid processes.

1. Introduction

Fast development of the world economy and increase of the international oil price have made the global energy and environmental problems increasingly serious. The supply of coal is much more abundant than that of oil; therefore, the development of coal-based technologies for producing clean fuel is very important for the sustainable development of the economy and of the energy supply for the world. Gas-to-liquid processes of Fischer−Tropsch (FT) synthesis, methanol synthesis, and dimethyl ether (DME) synthesis have become increasingly important and received much attention from both academic and industrial interests.[1−9] Besides providing clean fuel, the products of gas-to-liquid processes can be further produced to many other chemical products.[10]

Gas-to-liquid processes have the following common characteristics that must be considered in reactor design: (1) The reactions are strongly exothermic, with $-\Delta H_r = 165-204$ kJ/mol CO for FT synthesis, $-\Delta H_r = 90.3$ kJ/mol CO for methanol synthesis, and $-\Delta H_r = 102.2$ kJ/mol CO for DME synthesis. (2) The uniform profile of the temperature should be maintained because a nonuniform temperature profile and hot spots may cause a decrease in product selectivity and, more severely, cause catalyst deactivation. (3) Developing a large scale is critically important from the point view of the economy to produce low-priced fuel. (4) The processes are operated at high temperature and pressure. Corresponding to the above characteristics, the reactor must realize efficient and rapid removal of the accompanying large heat of reaction, maintain a uniform temperature profile, and be easy to scale up to large dimensions.

Great efforts have been devoted to reactor development to satisfy the requirements of different gas-to-liquid processes. Several reactor types are currently used for FT synthesis, methanol synthesis, and DME synthesis. For example, reactors for FT synthesis include the multitubular fixed bed, gas−solid fluidized bed, and slurry bubble column reactors.[1,3,11] For methanol synthesis and DME synthesis, the fixed bed, fluidized bed, slurry bubble column, and slurry airlift reactors were used or studied.[4,7−9,12,13] The differences between these several reactor types are largely related to different approaches to temperature control and the choice of catalyst.[14]

Although different reactor types were used for gas-to-liquid processes, the majority of attention during the past 10 years, from both academic and industrial interests, was paid to the slurry reactor. The slurry reactor presents the advanced reactor technology for gas-to-liquid processes. Its advantages include simple construction, excellent heat transfer performance, online catalyst addition and withdrawal, and reasonable interphase mass transfer rates with low energy input, which make it very suitable for gas-to-liquid processes. However, its multiphase flow behaviors are very complex and the multiphase reactor has some remarkable scale-up effects. Under industrial conditions, the high pressure, temperature, and solid concentration have notable and complex influences on the bubble behaviors, gas holdup, liquid velocity, and mass and heat transfer behaviors. Due to the presence of an additional liquid phase, gas−liquid mass transfer limitations in a gas−liquid−solid slurry system may cause a decrease in the reaction conversion, especially at high solid concentrations and superficial gas velocities. Further, the separation of fine catalyst particles from the viscous wax in FT synthesis is a challenging engineering problem. Therefore, extensive studies are still needed on the hydrodynamics, mass transfer, and liquid−solid separation for the development and design of high-performance slurry reactors for gas-to-liquid processes.

This article gives a state-of-the-art review of the studies on the slurry reactor for gas-to-liquid processes. It is organized as follows. In section 2, the historical and current development of

* To whom correspondence should be addressed. Tel.: +86-10-62797490. Fax: +86-10-62772051. E-mail: wangtf@flotu.org.

10.1021/ie070330t CCC: $37.00
Published on Web 08/02/2007

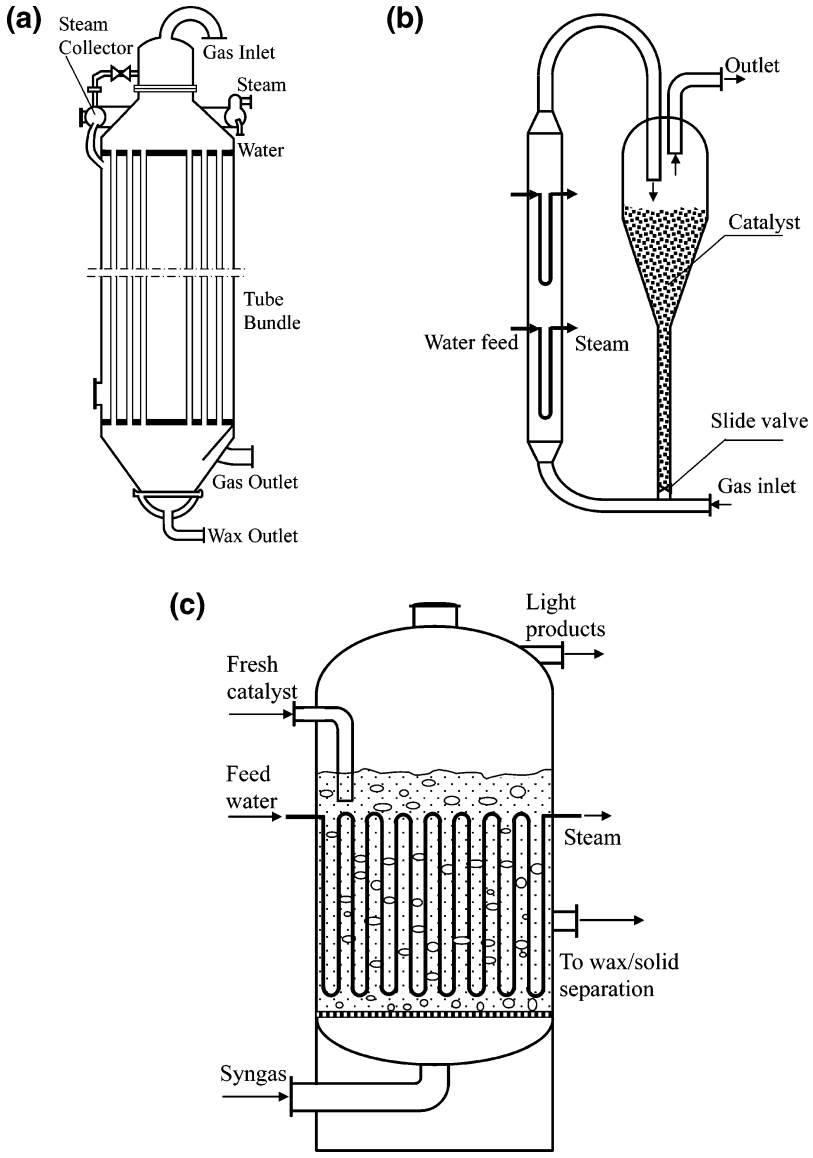

Figure 1. Reactor types used for FT synthesis. (a) Fixed bed reactor. (b) Circulating fluidized bed reactor. (c) Slurry buble column reactor.

slurry reactors for FT synthesis, DME synthesis, and methanol synthesis are overviewed. In section 3, studies on the slurry reactor are discussed in detail, including (1) *reactor type*, (2) *kinetics of gas-to-liquid processes*, (3) *flow regimes*, (4) *bubble behaviors, gas holdup, and liquid velocity*, (5) *mass transfer*, (6) *liquid−solid separation*, and (7) *hydrodynamics and mass transfer in slurry airlift reactors*. In section 4, process intensification by using internals is discussed. In section 5, modeling and simulations of gas−liquid and gas−liquid−solid multiphase flows are selectively reviewed, with focus on the new trend of coupling the population balance model (PBM) into the computational fluid dynamics (CFD) framework to describe the complex bubble behaviors and gas−liquid interphase interactions. In section 6, the results of a 3000 ton/year pilot plant for direct synthesis of DME in a slurry airlift reactor are given. The remarks and conclusions are given in the last section.

2. Slurry Reactor for Gas-to-Liquid Processes

Slurry reactors are extensively used in a variety of chemical, petrochemical, biochemical, and environmental processes for such as hydrogenation, oxidation, chlorination, hydroformylation, cell growth, and bioremediation.[15,16] Recently, slurry reactors have been considered as the advanced technology for gas-to-liquid processes. Their advantages include the following:[17,18] (1) simple construction and lower capital required for a large-scale slurry reactor; (2) good performance in temperature control; (3) feasibility for large capacity; (4) lower pressure loss that considerably saves the compression cost; (5) online removal and addition of catalyst; (6) lower catalyst amount than the fixed bed reactor due to high catalyst efficiency in a slurry reactor. As a result, there is a trend of shift from the fixed bed reactor to the slurry reactor in gas-to-liquid processes.[4,19]

2.1. Slurry Reactor for FT Synthesis. At present, the multitubular fixed bed reactor, gas−solid fluidized bed reactor, and gas−liquid−solid slurry reactor, as shown in Figure 1, are used for FT synthesis.[11,17,20,21] The reactor type and the operating conditions are the governing factors in the control of product distribution during FT synthesis. The multitubular fixed bed reactor and slurry reactor were used for the low-temperature process, while the circulating fluidized bed reactor and fixed fluidized bed rector were used for the high-temperature process.[21] The high-temperature process yields large amounts of olefins, a lower boiling range, and very good gasoline. Substantial amounts of oxygenates are also produced. The low-temperature process yields much more paraffin and linear products and can be adjusted to very high wax selectivity. The

primary diesel cut and wax cracking products can give excellent diesel fuels. The very linear primary gasoline fraction needs further treatment to attain a good octane number. Olefin and oxygenate levels for the low-temperature process are lower than those for the high-temperature process.

The fixed bed reactor for FT synthesis, such as the Arge reactor at Sasol, consists of a shell containing tubes packed with catalyst. Heat removal for the highly exothermic synthesis reaction is achieved by generation of steam on the shell side of the reactor. To replace the fixed bed reactor for the low-temperature FT process, the Sasol slurry reactor was developed.[17,21] In June 1991, Sasol decided to use the slurry reactor for its planned expansion of low-temperature FT capacity. A single slurry reactor, 5 m in diameter and 22 m in height, was commissioned in May 1993. Recently, it has been announced that Sasol and Phillips Petroleum have signed a memorandum of understanding with Qatar Geral Petroleum Corporation for a feasibility study on a 20 000 bbl/day plant for production of distillates and naphtha from Qatar's natural gas reserves, scheduled for startup in 2002. This plant was to make use of the slurry reactor technology.

The slurry reactor for FT synthesis has a number of advantages over the fixed bed reactor. It was reported that the capital required for a large-scale slurry reactor was less than 40% of that needed for an equivalent multitubular fixed bed reactor: The catalyst usage of the slurry reactor is about a third of that of the fixed bed reactor with a promise of even better performance, due to the catalyst's effectiveness and the higher average temperature used in the slurry reactor.[17] The slurry reactor has much better ability to be scaled up. The multitubular fixed bed is scaled up by increasing the number of tubes and the diameter of the reactor shell, and the large Arge multitubular fixed bed reactor was designed for about 1500 bbl/day. With the slurry reactor, capacity can be increased by increasing both the diameter and height of the reactor. It is thought feasible that a single slurry reactor with a capacity of about 10 000 bbl/day can be built.[17] Krishna and Sie compared the several reactor types for the FT synthesis process and concluded that the slurry reactor was the best reactor type for large-scale plants.[1] For the specific case of conversion of syngas into a relatively heavy FT product, de Swart et al.[22] compared the multitubular fixed bed reactor with the slurry reactor operating in either the homogeneous or heterogeneous regime. With a maximum weight of 900 ton/reactor as a limiting criterion, the number of reactors needed for a plant capacity of 5000 ton/day was found to be 10 for the multitubular fixed bed reactor, 17 for the slurry reactor operating in the homogeneous regime, and 4 for the slurry reactor operating in the heterogeneous regime.

2.2. Slurry Reactor for Methanol Synthesis. Similar to FT synthesis, one of the most difficult problems in designing a reactor for methanol synthesis is removing the heat of reaction while maintaining precise temperature control. This is important because catalyst life is seriously reduced by excessive temperatures. Tijm et al.[4] reviewed the development of the methanol process during the last decades. The reactor technologies that were extensively used in commercial plants for methanol synthesis fall into two categories, namely, the gas-phase technologies and liquid-phase technologies.

The gas-phase technologies operate in the gas phase using a fixed bed reactor with catalyst pellets, and many types of designs have been developed.[4,23] A Lurgi methanol reactor, as shown in Figure 2a, is a tube-based fixed bed that contains the catalysts in fixed tubes, and the reaction temperature is controlled by steam pressure. An ICI (Imperial Chemical Industries) methanol

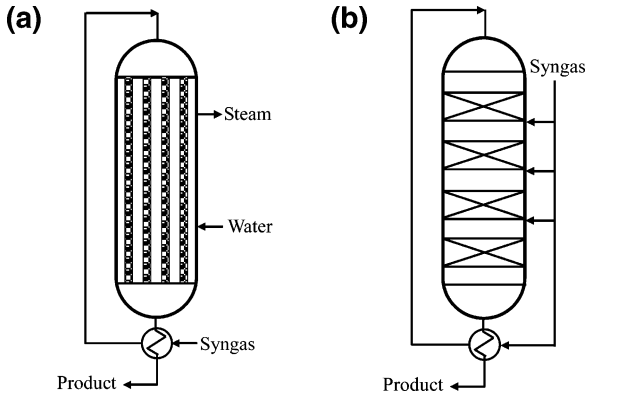

Figure 2. Fixed bed reactors for methanol synthesis. (a) Multitubular fixed bed. (b) Quench-cooled fixed bed.

reactor, as shown in Figure 2b, is an adiabatic reactor with cold unreacted gas injected between the catalyst beds to increase the once-through conversion of the synthesis reaction and lower the reaction temperature to extend the catalysts life. This quench-cooled design was also used by the Haldor Topsor methanol reactor and the TEC (Toyo Engineering Corporation) MRF-Z reactor.

Conversion of syngas to methanol in fixed bed reactors is limited by the reaction equilibrium and high-temperature sensitivity of the catalyst. Temperature moderation is achieved by recycling large amounts of hydrogen-rich gas, utilizing the heat capacity of H_2 gas and the higher gas velocities to enhance the heat transfer. To improve the heat transfer ability, Sherwin and Frank developed a liquid-phase process for methanol synthesis in which the mineral oil acted as a temperature moderator and facilitated heat removal by transferring the heat of reaction from the catalyst surface to boiling water in an internal tubular heat exchanger.[24] This liquid-phase process has a number of advantages: (1) the ability to operate with syngas rich in CO, as obtained from modern coal gasifiers, and produce a product that does not require further purification before being used as a fuel (It was reported that CO concentrations in excess of 50% have been routinely processed in the laboratory and at the Alternative Fuels Development Unit in LaPorte without any adverse effect on catalyst activity. In contrast, the fixed bed reactor must use a syngas rich in hydrogen. The gas-phase methanol technology that uses a fixed bed reactor requires such a feedstock to undergo stoichiometry adjustment by the water−gas shift reaction to increase the hydrogen content. Typically, a fixed bed reactor is limited to about 16% CO in the reactor inlet gas to limit the once-through conversion to avoid excess heating.); (2) enhanced heat transfer of the highly exothermic heat of reaction; (3) a high once-through conversion of CO. In the liquid−phase process, the heat transfer coefficient on the slurry side of the heat exchanger is relatively large.[25−27] Thus, a relatively small heat transfer area is required, and the heat exchanger occupies only a small fraction of the cross-sectional area of the reactor. Further, the heat transfer between the solid catalyst and the liquid phase is highly efficient, thereby allowing high once-through conversions without loss of catalyst activity.

The LPMEOH technology, developed by Air Products has been tested for several years at a pilot plant of 10 short ton/day owned by the U.S. Department of Energy at La Porte, Texas. To demonstrate the scale-up of the slurry reactor from 10 to 260 short ton/day, operation of a commercial-scale demonstration of the LPMEOH process was started in 1997, at Eastman's chemicals-from-coal complex in Kinsport, Tennessee. The results of the demonstration process were satisfactory and verified the advantages of the slurry reactor.

2.3. Slurry Reactor for DME Synthesis. DME was conventionally used for such applications as cosmetics and aerosol paint propellants. The mostly used reactor for DME synthesis was the fixed bed reactor. In recent years, DME has been considered a clean and economical alternative fuel of household, transportation, and power generation, because of its much smaller environmental impact. The efficient synthesis of DME from syngas that can be derived from coal, natural gas, or biomass has received much attention. To be used as a fuel, DME must be produced in large quantities and at a low cost. It is more important to control the reaction temperature for DME synthesis than for methanol synthesis, because the equilibrium conversion of DME synthesis is higher than that of methanol synthesis.

The direct synthesis of DME from syngas by dual function catalysts has been studied during the past decades. The synthesis of DME in a single reactor is based on a combination of an equilibrium-limited methanol synthesis reaction and an equilibrium-unlimited methanol dehydration reaction.[28] The direct synthesis of DME from syngas in a slurry reactor, developed by Air Products,[12] by JFE Corporation,[7] and by Tsinghua University,[9] is now considered the most promising DME synthesis technology. JFE and Air Products used a slurry bubble column reactor, while the technology developed by Tsinghua University used a slurry airlift reactor with internals in the riser.

JFE collaborating with Taiheiyo Coal Mining Co., Sumitomo Metal Industry Ltd., and the Center for Coal Utilization, Japan, finished a project of a 5 ton/day pilot plant in 2001 and obtained satisfactory results.[7] On the basis of this achievement, DME Development Co. Ltd. started a 100 ton/day demonstration plant project at Hokkaido, Japan, in 2002. Air products carried out a 25-day test of the LPDME process in the La Porte Alternative Fuels Development Unit of 10 short ton/day to evaluate the production of DME as a coproduct with methanol. This test showed promise, but no DME runs were made in the demonstration LPMEOH reactor of 260 short ton/day at Kingsport. Tsinghua University began to study the DME synthesis process in 1998 and, in 2002, cooperating with Chongqing Yingli Fuels & Chemicals Co. Ltd., began a 10 ton/day pilot plant project. The pilot plant was run in 2004, and expected results were obtained.

Direct synthesis of DME in a single reactor makes the synthesis process simpler and more compact than the two-step process. Further, the limitation of thermodynamic equilibrium to methanol synthesis is overcome through shifting the equilibrium by converting methanol to DME. Therefore, a higher once-through conversion of CO can be obtained. Due to the synergy effect of process coupling, syngas rich in CO can be used as the feedstock for DME synthesis, and the steam and water−gas shift reaction system can be saved. These will further reduce the investment and production cost.[29]

3. Studies on Slurry Reactors

The discussion above shows that slurry reactors have become the advanced technology for gas-to-liquid processes. Although relatively simple in construction, slurry reactors are still difficult to design and scale-up due to the lack of detailed information on hydrodynamics and mass transfer over a wide range of industrial operating conditions.[18] For design and scale-up, predictions of the gas holdup, liquid flow pattern, gas−liquid mass transfer rate, and heat transfer rate are desired. Knowledge of the bubble size distribution, coalescence, and breakup behaviors is also important, since the bubble behaviors are closely related to the hydrodynamics and heat and mass transfer.

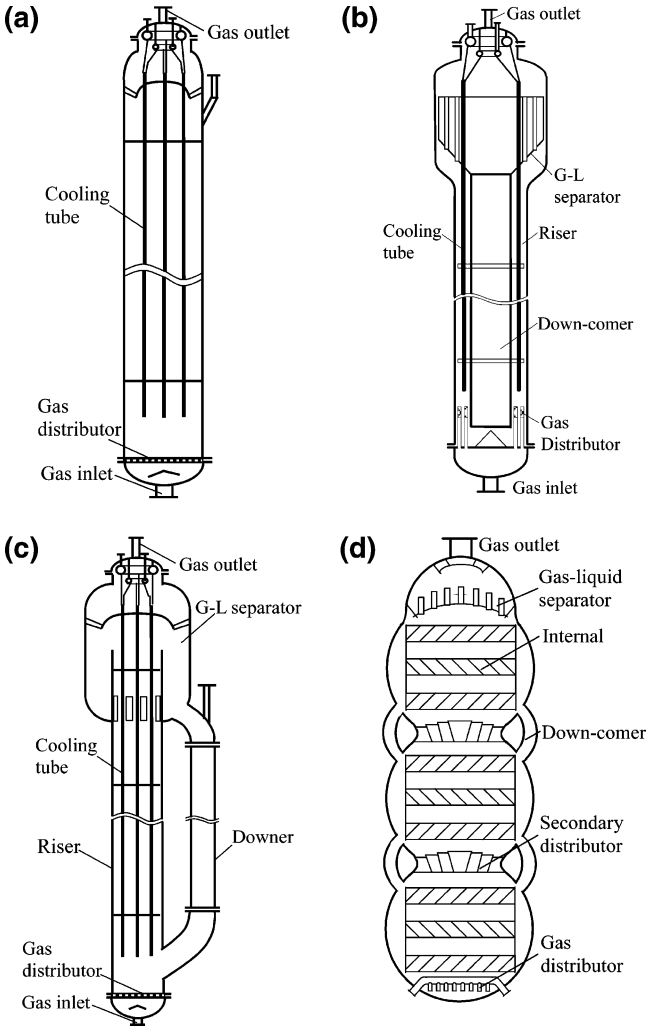

Figure 3. Types of slurry reactors. (a) Bubble column. (b) Internal-loop airlift reactor. (c) External-loop airlift reactor. (d) Spherical reactor.

Further, the following issues must be addressed for development and design of a slurry reactor for gas-to-liquid processes: (1) The reactor should operate at a high superficial gas velocity and a high solid concentration, thus in the typical heterogeneous regime, to get an increased volumetric productivity.[30,31] However, the hydrodynamics and mass and heat transfer behaviors in the heterogeneous regime are much more complex than in the homogeneous regime, and studies on this flow regime are still limited. (2) The influences of the temperature and pressure must be reliably predicted since all slurry reactors for gas-to-liquid processes operate under conditions of high temperature and pressure. (3) The gas−liquid mass transfer limitation may cause a decrease in the reaction conversion, especially at high solid concentrations and superficial gas velocities. (4) The gas distributor may affect the stable operation of the reactor[8] and requires a proper design for robust and efficient performance. (5) In the case of FT synthesis, the separation of fine particles from wax is difficult and requires special treatments.

In the following part, studies on the slurry reactor will be selectively reviewed, with focus on issues related to design and scale-up of an industrial-scale reactors for gas-to-liquid processes.

3.1. Reactor Type. Slurry reactors include the bubble column, internal-loop airlift reactor, external-loop airlift reactor, and spherical reactor, as shown in Figure 3a−d. Different from the bubble column, the airlift reactor consists of riser and downcomer that provide the flowing channel for global circulation

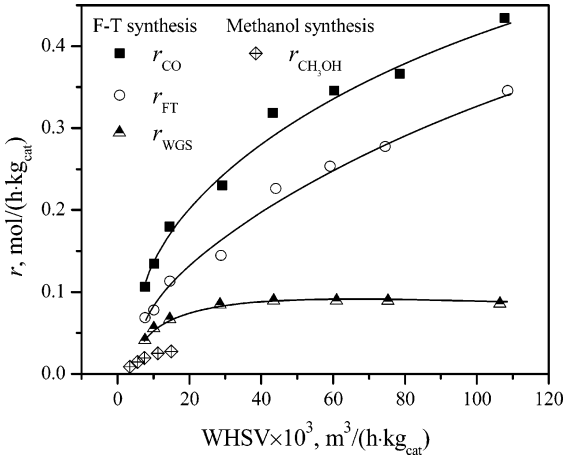

Figure 4. Typical reaction rates for FT synthesis and methanol synthesis in a slurry system. For FT synthesis, H_2/CO feed ratio = 1.7, T = 270 °C, P = 1.308 MPa, and data is from the work of Raje and Davis.[35] For CH_3-OH synthesis, H_2:CO:CO_2 = 50.9:39.5:4.7, T = 230 °C, P = 3.45 MPa, and data is from the work of Šetinc and Levec.[33]

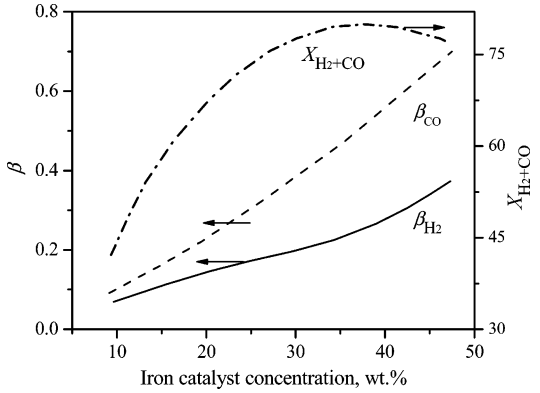

Figure 5. Effect of catalyst concentration on β and (H_2 + CO) conversion. β is defined as $(1/k_l a)/[1/k_l a + 1/k_o(\phi_i)]$, in which k_o is the overall kinetics rate constant. This figure has been adapted from the work of Inga and Morsi.[38]

of the liquid−solid slurry phase. With the consideration that the manufacture of large cylindrical reactors (such as those 6−10 m in diameter) operating at high pressure (such as 10 MPa) is very difficult, Jin et al.[32] proposed a novel spherical reactor with relatively thin wall. The spherical reactor has higher mechanical resistance to pressure than the cylindrical column and, thus, decreases the wall thickness and reactor cost. Comparing the cylindrical and spherical reactors of the same volume and at the same pressure, the advantages of the spherical reactor can be seen from the following parameters: reactor surface ratio $F_s/F_c = 0.875$; wall thickness ratio $\delta_s/\delta_c = 0.5$; reactor weight ratio $W_s/W_c = 0.437$; reactor price ratio $\$_s/\$_c \approx W_s/W_c = 0.437$. Further, in a reactor consisting of multiple spherical units with novel internals, not only can the distribution of local parameters be uniform in the radial direction, but also the liquid-phase back-mixing can be effectively decreased. The spherical reactor has economical feasibility and the great potential for large-scale production in the gas-to-liquid processes.

3.2. Kinetics of Gas-to-Liquid Processes. Although this review focuses on the engineering aspects of the slurry reactor for the gas-to-liquid processes, the reaction kinetics is first discussed briefly here with the consideration that the reaction kinetics is fundamental to the process and provides the basis for why physical effects, such as mass and heat transfer, mixing, etc., must be studied. Reviews on the reaction kinetics for the gas-to-liquid processes are available in the literature. Cybulski,[25] Šetinc and Levec[33] reviewed the kinetics of liquid-phase methanol synthesis. Van der Laan and Beenackers reviewed the kinetics and selectivity of the FT synthesis.[34] The FT synthesis can be simplified as a combination of the FT reaction and the water−gas shift reaction (WGS): (1 FT) $CO + (1 + n/2)H_2 \rightarrow CH_n + H_2O$; (2 WGS) $CO + H_2O \rightarrow CO_2 + H_2$. And, the reaction rates satisfy $r_{FT} = -r_{CO} - r_{WGS}$. Figure 4 shows typical values of the reaction rates, r_{FT} and r_{WGS}, in a slurry system. Typical reaction rates of methanol synthesis are also shown in Figure 4 for comparison.

It was reported that, in the FT slurry process, only the resistances of reaction kinetics and gas−liquid mass transfer were significant.[36,37] Thus, quantitative comparison between the gas−liquid mass transfer and reaction kinetics is important for optimum design and operation of the reactor. Satterfield and Huff[36] claimed that FT synthesis was severely controlled by gas−liquid mass transfer, particularly at high temperatures. Deckwer et al.,[37] however, reported that the gas−liquid mass transfer resistance represented less than 20% of the total resistance. proposed an approach to determine the rate-limiting step in the FT slurry process, in which the water−gas shift (WGS) reaction was taken into account and the "singular kinetic path" concept was used.[38] They defined the relative extent of the gas−liquid mass transfer resistance β as $(1/k_l a)/[1/k_l a + 1/k_o(\phi_i)]$, in which k_o is the overall kinetics rate constant. Figure 5 showed the influence of the catalyst concentration on β as well as (CO + H_2) conversion.[38] The FT synthesis in a slurry system using the commercial iron-based catalysts could be considered a reaction kinetics-controlled process. The reactor performance could be improved by increasing the catalyst activity or catalyst concentration up to a maximum of 37−40 wt %. In both cases, the reactor would approach a mass transfer-controlled regime, especially at high catalyst concentration which would markedly increase the bubble size. From the results of Inga and Morsi,[38] it can be seen that although the resistance of reaction kinetics is larger than that of mass transfer, these two resistances are on the same order of magnitude. Thus, intensification of the gas−liquid mass transfer can increase the conversion and increase the critical catalyst concentration at which maximum conversion is obtained.

3.3. Flow Regimes. The hydrodynamics in a gas−liquid or gas−liquid−solid reactor are characterized by different flow regimes, namely, the homogeneous, transition, and heterogeneous regimes, mainly depending on the superficial gas velocity. The homogeneous regime exists at low superficial gas velocities and changes to the heterogeneous regime with an increase in the superficial gas velocity. The industrial interest for gas-to-liquid processes is in the heterogeneous flow regime.[1,39] The hydrodynamics, heat and mass transfer, and mixing behavior are quite different in different regimes.[40] It is therefore extremely important to understand the different hydrodynamics and flow regime transitions for the purpose of reactor design, operation, control, and scale-up.

Much work has been done to study the regime transition in multiphase flows in the last decades, and several experimental approaches for identifying flow regime transition have been proposed. These approaches generally fall into two types: one type is based on a sharp variation of the gas holdup[40] or the drift flux[41,42] with respect to the superficial gas velocity or uses the dynamic gas disengagement technique; the other type is based on analysis of the dynamic signal-by-signal processing methods such as statistical analysis,[43,44] fractal analysis,[45] and chaotic analysis.[46] In recent years, regime identification methods based on theoretical analysis, such as linear analysis[47] and the population balance model,[48] were also developed. Table 1

Table 1. Comparison of Methods for Identifying the Flow Regime Transition[a]

	advantages and disadvantages[b]				
method	application	accuracy	ease of use	comp. cost	additional information
$\alpha_g - U_g$ plot method	BC	☆,×[c]	☆	☆	gas holdup
drift-flux method	ALR	○	☆	☆	gas holdup, and C_0 (related to radial profile), C_1(related to bubble rise velocity)
DGD method	BC	○	○	☆	flow structure of the gas phase, bubble rise velocity
fractal approach	BC & ALR	○	○	×	Hurst exponent and fractal dimension
chaos analysis	BC & ALR	☆	○	×	correlation dimension and Kolmogorov entropy
statistical analysis	BC & ALR	○	○	○	probability density function (PDF) of the signal and the moments of PDF
autocorrelation function	BC & ALR	☆	○	○	characteristic scales of time and length
population balance model	BC & ALR[d]	○[e]	○	×	bubble breakup and coalescence rate and flow structure of the gas phase

[a] Part of this table was adapted from the results of Vial et al.[55] [b] Symbols used in the table have the following meaning: (☆) good, (○) medium, (×) poor. [c] ☆ when the plot has a maximum and × otherwise. [d] In principle, the PBM can be used to identify the flow regime transition in ALR as well, but related results have not yet been reported in the literature. [e] The accuracy strongly depends on the bubble breakup and coalescence modeling.

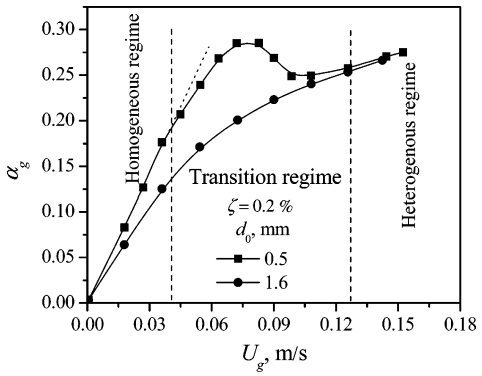

Figure 6. Identification of regime transition with the $\alpha_g - U_g$ plot method reprinted with permission from the work of Zahradník et al.[40] Copyright 1996 Elsevier Limited.

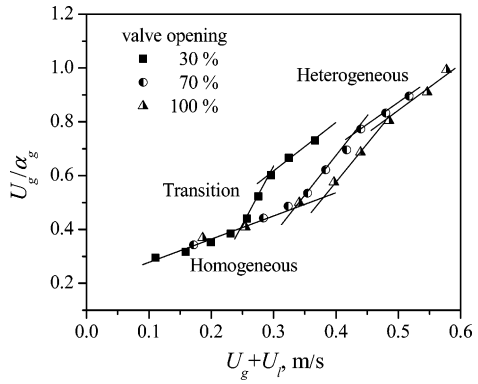

Figure 7. Identification of regime transition with the drift-flux model reprinted with permission from the work of Vial et al.[42] Copyright 1992 Elsevier Limited.

summarized the advantages and disadvantages of the typical methods for identifying the flow regime transition in terms of application range, accuracy, ease of use, computational cost, and additional information provided.

3.3.1. $\alpha_g - U_g$ Plot Method. The method of identifying flow regime transition by plotting the gas holdup, α_g, with respect to the superficial gas velocity, U_g, is based on the different variation of α_g with increasing U_g, as shown in Figure 6. In the homogeneous regime, the gas holdup shows an approximate linear increase with increasing superficial gas velocity; when the flow enters the heterogeneous regime, the increase of the gas holdup with increasing superficial gas velocity becomes less pronounced. Therefore, the slope of the $\alpha_g - U_g$ plot can be used to identify the flow regime. With an efficient gas distributor, such as a sintered porous plate or perforated plate with small orifices, the flow exhibits typical homogeneous, transition and heterogeneous regimes with increasing superficial gas velocity;[40,49,50] while with a gas distributor of poor performance, such as a single nozzle or perforated plate with relatively large orifices, the heterogeneous regime prevails even in low superficial gas velocities.[49]

3.3.2. Drift-Flux Method. The drift-flux model, proposed by Zuber and Findlay,[41] is expressed as follows:

$$U_g/\alpha_g = C_0(U_g + U_l) + C_1$$

where C_0 is a parameter related to radial uniformity of the gas holdup and C_1 is a parameter related to the bubble rise velocity. Because the radial profiles of the gas holdup are different in the homogeneous and heterogeneous regimes, the variation of C_0 with $U_g + U_l$ can be used to identify the flow regime transition, as shown in Figure 7.[42]

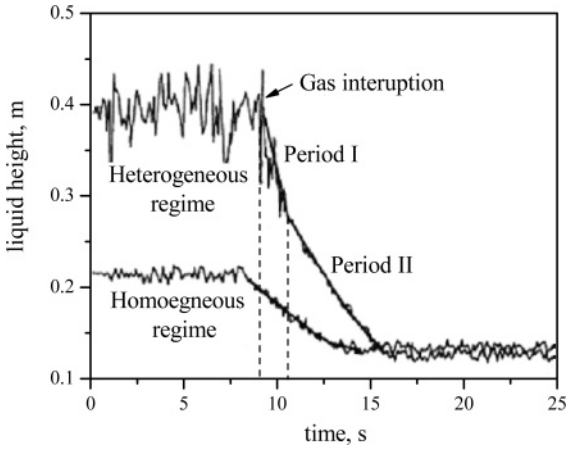

Figure 8. Identification of regime transition with the DGD method reprinted with permission from the work of Camarasa et al.[49] Copyright 1999 Elsevier Limited.

3.3.3. Dynamic Gas Disengagement (DGD) Method. The DGD method was initially proposed by Sriram and Mann[51] and has been widely used to study the bubble holdup structure and bubble rise velocities.[39,49,52,53] In the DGD method, the gas supply is sharply stopped and the gas holdup variation is monitored. The variation of the gas holdup shows different characteristics in different flow regimes, as shown in Figure 8. In the homogeneous regime, the gas holdup decreases linearly with lapsing time after stopping the gas supply. In the heterogeneous regime, the variation of the gas holdup with lapsing time has two different periods: in the first period, both large bubbles and small bubbles disengage from the liquid, resulting in a much faster decrease in the gas holdup; while, in

the second period, all large bubbles have disengaged from the system and only small bubbles disengage from the liquid, resulting in a slower decrease in the gas holdup.

3.3.4. Dynamic Signal Analysis Method. Drahoš et al.[43] analyzed the pressure fluctuations by a fractal approach and found that the value of the Hurst exponent computed from the rescaled range analysis could be used to distinguish the flow regime transition. Bakshi et al.[54] studied the regime transition in a gas−liquid bubble column using multiresolution analysis of the gas holdup signal and found that the intermittence of the measured signal characterized the transition from the homogeneous to heterogeneous regime. Letzel et al.[46] used the chaotic invariant Kolmogorov entropy to quantify the chaos dynamics in bubble columns, and showed that Kolmogorov entropy indicates a sharp transition from the homogeneous to heterogeneous regime. Vial et al.[55] compared several methods of regime identification based on analysis of pressure fluctuations, including statistical analysis, spectral analysis, fractal analysis, chaotic analysis, and time−frequency analysis, both in a bubble column and an external-loop airlift reactor. Their ability to determine regime transition and to extract regime features is compared. A new simple and efficient method was proposed for regime identification based on the autocorrelation function. This method also provided quantitative information about the characteristic time and the axial dimension of the flow structure. Lin et al.[56] estimated four chaotic invariants, namely, correlation dimension, largest Lyapunov exponent, metric entropy, and mutual information in different flow regimes. The transition superficial gas velocity was determined by the sharp increase or decrease of these obtained chaotic invariants.

3.3.5. Population Balance Model Method. The above approaches need experimental data and do not give a direct explanation on the mechanism of regime transition. Due to the complexity of gas−liquid flows, it is very difficult to predict the regime transition by theoretical modeling. Olmos et al.[57] modeled the gas−liquid flow with the population balance model (PBM), and the results showed that it was possible to predict numerically the regime transition as long as several gas phases were considered. In their work, 10 bubble classes of diameters ranging from 1 to 10 mm were used. This bubble division may cause remarkable errors because bubbles much larger than 10 mm exist in the heterogeneous regime. The authors pointed out that their study did not pretend to describe exactly the complex coalescence and breakup phenomena occurring in bubble columns but rather showed the possibilities of the application of population balance equations. They used the bubble breakup and coalescence kernels proposed by Luo and Svendsen[58,59] and Prince and Blanch,[60] respectively. However, these bubble breakup and coalescence models have some limitations.[61−63] Furthermore, it is necessary to consider the multiple bubble breakup and coalescence mechanisms to reasonably predict the bubble size distribution both in the homogeneous and heterogeneous regimes.[48,63]

Wang et al.[48] studied the theoretical prediction of flow regime transition in bubble columns based on the bubble size distribution predicted by the PBM with 30 bubble classes (from 0.0576 to 11.6 cm). Models for bubble coalescence and breakup resulted from different mechanisms, including coalescence resulting from turbulent eddies, coalescence resulting from different bubble rise velocities, coalescence resulting from bubble wake entrainment, breakup resulting from eddy collision, and breakup resulting from large bubble instability, were proposed. Simulation results in Figure 9 showed that, at relatively low superficial gas velocities, bubble coalescence and breakup were relatively

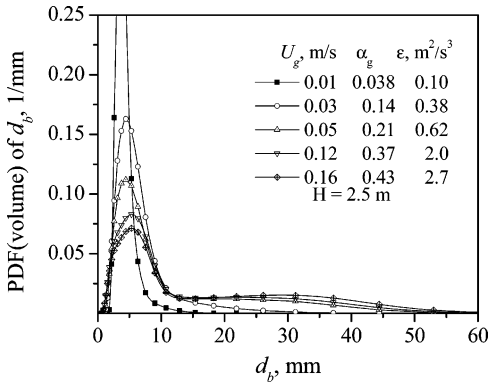

Figure 9. Bubble size distribution in different superficial gas velocities predicted by PBM reprinted with permission from the work of Wang et al.[48] Copyright 2005 Elsevier Limited.

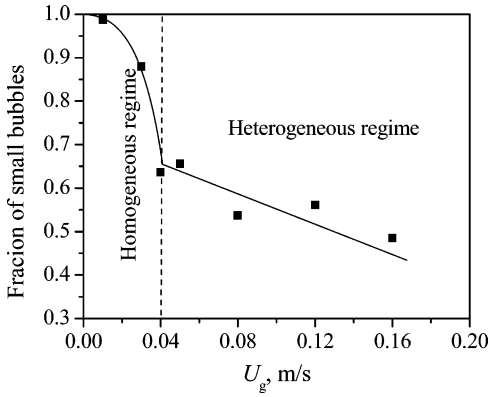

Figure 10. Variation of the volume fraction of small bubbles with respect to superficial gas velocity predicted by PBM reprinted with permission from the work of Wang et al.[48] Copyright 2005 Elsevier Limited.

weak and the bubble size was small and had a narrow distribution; with an increase in the superficial gas velocity, large bubbles began to form due to bubble coalescence, resulting in a much wider bubble size distribution. The regime transition was predicted to occur when the volume fraction of small bubbles sharply decreased, as shown in Figure 10. The predicted transition superficial gas velocity was about 4 cm/s for the air−water system, in accordance with the values obtained from experimental approaches.

3.4. Bubble Behaviors, Gas Holdup, and Liquid Velocity. Bubble behaviors, gas holdup, and liquid velocity are the most important hydrodynamic parameters in a gas−liquid−solid slurry reactor. For measuring techniques for experimental study on the hydrodynamics in gas−liquid and gas−liquid−solid multiphase reactors, readers are referred to the comprehensive review by Boyer et al.[64] Early studies on the slurry reactor focused on the global hydrodynamic behaviors, while the local parameters, such as the gas holdup, liquid velocity, bubble size, and rise velocity, are useful for a better understanding of the hydrodynamics in the reactor. However, experimental studies on local hydrodynamic parameters are still limited, mainly due to the difficulty with the experiment and measuring technique. In recent years, more and more studies on local hydrodynamic behaviors have been reported[65−69] and resulted in a much better understanding of the slurry reactor. The dominant conditions that influence the hydrodynamics and mass and heat transfer behaviors include the superficial gas velocity, pressure, temperature, solid concentration, reactor dimensions, and gas distribution.

3.4.1. Influence of Superficial Gas Velocity. 3.4.1.1. Influence of U_g on Bubble Behavior. In low superficial gas velocities, bubbles are relatively small and uniform with weak bubble−bubble interaction. In high superficial gas velocities, bubble breakup and coalescence become significant, resulting in a wide bubble size distribution. For simplification, bubbles in the heterogeneous regime were often divided into two groups of small and large bubbles and were studied with the DGD method.[39,49,52,53] The coexistence of small and large bubbles in gas−liquid and gas−liquid−solid reactors have been found by visual observation.[70,71] It should be pointed out that the existing DGD models, without considering the bubble−wake attraction effect, may severely underestimate the holdup of small bubbles and overestimate the holdup of large bubbles, especially in high superficial gas velocities.[72] In recent years, the PBM was used to predict the bubble size distribution.[48,57,63,73−75] Although much work remains to be done with the PBM method, it provides a theoretical framework in which to study the complex bubble behaviors and has drawn increasing attention in recent years.

Generally speaking, the bubble size increases with increasing superficial gas velocity. Fukuma et al.[76] and Saxena et al.[77] reported that the bubble size increased with increasing superficial gas velocity and the maximum bubble size was attained at a certain gas velocity. Similarly, Li and Prakash reported that the bubble size increased with increasing superficial gas velocity.[53] However, contrary results have been reported in relatively low superficial gas velocities.[78,79] This contradiction may rise from differences in the gas distributor.

In the homogeneous regime, the bubble rise velocity almost does not change with the superficial gas velocity. In the heterogeneous regime, the bubble rise velocity is much more complex. DGD experiments showed that the rise velocity of small bubbles decreased whereas the rise velocity of large bubbles increased with increasing superficial gas velocity.[53,80] Schumpe and Grund[81] obtained similar results except they found that the rise velocity of small bubbles decreased gradually with increasing superficial gas velocity and attained an almost constant value afterward.

In the homogeneous regime, the bubble behaviors are fairly uniform in the radial direction. While in the heterogeneous regime, enhanced bubble coalescence results in a wide bubble size distribution and an increasing radial nonuniformity of the bubble behaviors. Experimental studies and numerical simulations showed that large bubbles rose up mainly in the central region of the column and with large rise velocities, while the radial profile of small bubbles is much more uniform.[74,82]

3.4.1.2. Influence of U_g on Gas Holdup. The superficial gas velocity is a dominant factor that affects the gas holdup, and numerous experimental studies have been reported.[39,52,67−69,83−85] Generally, the gas holdup increases with an increase in the superficial gas velocity, but this increase shows different characteristics in the homogeneous and heterogeneous regimes:[67,85] the average gas holdup increases almost linearly with increasing superficial gas velocity in the homogeneous regime, while this increase is less pronounced in the heterogeneous regime, because large bubbles are formed due to bubble coalescence and these large bubbles have a notable bubble−wake attraction effect.[74,86]

On the basis of the DGD experimental results, Krishna et al.[87,88] proposed a two-class bubble model, which has been widely used in studies on the heterogeneous regime. Krishna et al.[52] and Hyndman et al.[39] found that in the heterogeneous regime the overall gas holdup increased with increasing superficial gas velocity, mainly due to an increase in the large-bubble holdup; the contribution of small bubbles to the overall gas holdup was almost constant and equal to the transition holdup, i.e., it did not increase with increasing superficial gas velocity.

The radial profile of the gas holdup is relatively uniform in the homogeneous regime and becomes more parabolic in the heterogeneous regime.[85,89−91] This difference has been explained with the lateral forces that act on the bubbles.[74,84,92−94] The radial profile of the gas holdup is determined by such lateral forces as the transverse lift force, turbulent dispersion force, and wall lubrication force. These lateral forces depend on the bubble size, for example, the transverse lift force acts to the high-liquid-velocity side for large bubbles and to the low-liquid-velocity side for small bubbles. The bubble size distributions in the homogeneous and heterogeneous regimes are much different, and thus, the gas holdup also shows different radial profiles.

3.4.1.3. Influence of U_g on Liquid Velocity. In the bubble column, the liquid rises with the bubbles in the central region of the column and flows downward in the near-wall region. In fact, the radial profiles of the gas holdup and liquid velocity are closely related to each other.[95] The value of the center-line liquid velocity, u_{l0}, increases with increasing superficial gas velocity.[67,89,96,97] Degaleesan et al. studied the radial profiles of the time-averaged nondimensional axial liquid velocity, $<u_l>/U_g$, for three columns of different size.[67] Their results showed that the variation of the liquid velocity with respect to the superficial gas velocity depended on both the flow regime and column diameter. In the 14 cm column, the radial profiles of $<u_l>/U_g$ fell into two groups: one for U_g values of 2.4 and 4.8 cm/s, and the other for U_g values of 9.6 and 12 cm/s. These two group clearly represented the homogeneous and heterogeneous regimes, respectively. A similar trend was observed in the 19 cm column, while the radial profiles of $<u_l>/U_g$ for the 44 cm column did not overlap. Wu and Al-Dahhan proposed a correlation, which involved two parameters of the radial profile of the gas holdup, for prediction of the radial profile of the axial liquid velocity. This correlation required as input only the superficial gas velocity, physical properties, and column dimensions.[95] The value of u_{l0} was recommended to be obtained from either experiments or correlations by Zehner[98] and Riquarts.[99] In their work, the experimental value of u_{l0} was used and good agreement was obtained compared with the radial profiles of the measured liquid velocity reported in the literature within a wide range of conditions. However, the prediction of u_{l0} is rather difficult. Krishna et al. made a comparison of nine correlations for u_{l0} in the air−water system and found that there was a very large discrepancy among the predictions.[100] Their results also showed that full CFD simulations could give reliable predictions of radial profiles of the liquid velocity.

3.4.2. Influence of Physical Properties. Zahradník et al.[83] studied the influence of the liquid viscosity on the gas holdup and regime transition in an aqueous saccharose solution in a bubble column using a perforated plate gas distributor with 0.5 mm orifices. They found that the gas holdup remarkably decreased with increasing liquid viscosity, as shown in Figure 11. With liquids of low viscosity, the dependence of the gas holdup on the superficial gas velocity exhibited a typical maximum or plateau that characterized the existence of the homogeneous regime and its transition to the heterogeneous regime. Above a critical value of liquid viscosity, say 8.0 mPa·s, formation of the homogeneous regime was suppressed and the flow was in the heterogeneous regime. Li and Prakash[101] and Urseanu et al.[102] also found a decrease in the gas holdup with increasing liquid viscosity. Kuncová and

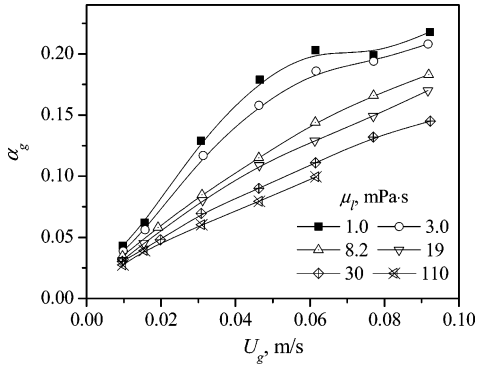

Figure 11. Influence of liquid viscosity on gas holdup reprinted with permission from the work of Zahradník et al.[83] Copyright 1997 Elsevier Limited.

Zahradník[103] obtained similar results in a bubble column reactor 0.152 m in diameter using aqueous solutions of saccharose within the viscosity range 1−l10 mPa·s, but the dependence of gas holdup on liquid viscosity exhibited a slight maximum at $\mu_l \approx 3$ mPa·s, followed by a sustained decrease of gas holdup with increasing viscosity up to $\mu_l \approx 30$ mPa·s.

It was also reported that adding a small amount of a surface-acting material (surfactant) to water resulted in a decrease in the bubble size and significantly higher gas holdup values.[104−106] Zahradník et al.[105] studied the effect of the addition of aliphatic alcohols on the flow behavior in a bubble column with viscous liquid and found that the addition of a relatively small amount of alcohols ($c_A \cong 10^{-5}-10^{-2}$ kmol/m^3, with a smaller value for a longer carbon chain) had a significant effect on suppressing bubble coalescence, improving the radial uniformity of the gas holdup and increasing the gas holdup. Addition of alcohols compensated even for the negative effect of liquid viscosity on the formation and stability of the homogeneous regime. Dargar and Macchi[106] studied the effect of surface-active agents on the phase holdups of a gas−liquid bubble column and three-phase fluidized bed (with glass beads of 1.2 and 5.0 mm). The results showed that the presence of surface-active agents increased the gas holdups in a bubble column by an average of 41% and increased the gas holdups in a three-phase fluidized bed by an average of 37%. The presence of electrolyte or impurities were also found to increase the gas holdup.[107,108]

Veera et al.[109,110] studied the effect of addition of *n*-butanol on the gas holdup profiles with both multipoint and single-point spargers. They found that the solutions exhibited foaming behavior at higher concentrations of *n*-butanol and that the radial profile of the gas holdup depended strongly on the sparger design and the concentration of the alcohol. For both the multipoint and single-point spargers, the average gas holdup increased and the radial profiles of the gas holdup were flatter with an increase in the concentration of *n*-butanol.

3.4.3. Influence of Pressure. All the gas-to-liquid processes are carried out in high pressure and temperature. The hydrodynamics and mass transfer in such conditions are quite different compared with those in ambient conditions.[111] Although studies conducted at high pressure and temperature are much less abundant than those conducted at ambient conditions and the mechanism of pressure influence is not yet well understood, many valuable results have been obtained in the literature.

3.4.3.1. Influence of *P* on Bubble Behaviors. The influence of pressure on the initial bubble size depends on the dimensionless capacitance number of the chamber, defined as $N_c = 4V_c g\rho_l/\pi d_0^2 P$, where V_c is volume of the gas chamber and d_0 is the orifice diameter. When the pressure is low so that $N_c > 1$, the initial bubble size remarkably decreases with increasing pressure. When the pressure exceeds a value that makes $N_c < 1$, the increase of initial bubble size becomes insignificant with a further increase in the pressure.[111] For a given bubble size, the rise velocity of a single bubble decreases with increasing pressure, and the influence of pressure on the variation of u_b with d_b can be represented by the Fan−Tsuchiya equation.[112] Compared with low pressures, the number of large bubbles is reduced at high pressures and the bubble size distribution becomes narrower.[113−115] By visual observation, Lin et al.[71] found that the bubble size in the slurry reactor remarkably decreased with increasing pressure.

3.4.3.2. Influence of *P* on Gas Holdup. Experimental results showed that the gas holdup was uniquely dependent on the gas density no matter whether the increased gas density was a result of higher pressure or gas molecular weight.[87,114,116] Therefore, the gas density was used to describe the influences of both pressure and gas molecular weight.

It is suggested from the literature that the influence of gas density on the gas holdup is more remarkable at higher superficial gas velocities.[71,85,91,102,114,116−119] Actually, the gas holdup is almost independent of gas molecular weight or operating pressure in the homogeneous regime.[91,117,120] This explains the inconsistency of results concerning the influence of pressure on the gas holdup: some researchers reported an increase in the gas holdup with increasing pressure, while others found little influence of pressure on the gas holdup. Deckwer et al.[120] studied the influence of pressure on the gas holdup in the typical homogeneous regime and found the gas holdup to be independent of the pressure. Some other researchers[91,114,116,117] studied the influence of the pressure on the gas holdup in a wider superficial gas velocity range and found that, with an increase in the gas density, the gas holdup increased notably in high superficial gas velocities but had different variations in low superficial gas velocities, depending on the gas distributor, liquid viscosity, and solid concentration. When an efficient gas distributor, e.g., sintered plate or perforated plate with orifices smaller than 1.0 mm, is used, the typical homogeneous regime exists in which the gas density has negligible influence on the gas holdup.[91,117] With inefficient gas distributors such as a single nozzle or perforated plate with relatively larger orifices[49,71] or in a system with highly viscous liquid[102] or high solid concentration,[121] the heterogeneous regime prevails even in low superficial gas velocities. In such cases, the gas holdup increases with increasing gas density in low superficial gas velocities, but in a less pronounced manner than in high superficial gas velocities. Jiang et al.[122] reported that the gas holdup increased with increasing pressure up to a point, beyond which there was no significant pressure effect on the gas holdup. As discussed earlier, the transition superficial gas velocity increases with increasing pressure. When this transition velocity is larger than the operating superficial gas velocity, a further increase in the pressure will no longer have any influence on the gas holdup. Urseanu et al.[102] studied the influence of operating pressure on the gas holdup with different liquid viscosities. They found that the total gas holdup increased strongly with increasing pressure for a low-liquid-viscosity system (nitrogen−water, $\mu_l = 0.001$ Pa·s) and this increase was much less pronounced for the high-liquid-viscosity system (nitrogen−Tellus oil, $\mu_l = 0.07$ Pa·s); for extremely viscous systems ($\mu_l > 0.1$ Pa·s), the influence of pressure became insignificant.

The increase of the gas holdup with increasing gas density is mainly caused by the reduced stability of large bubbles, which, in turn, has two influences: One is that transition from the

homogeneous to heterogeneous regime is delayed, and the gas holdup at the transition point is also higher;[85,102,116,123] The other is that breakup of large bubbles is enhanced,[114] resulting in a decrease in the large-bubble size and an increase in the large-bubble holdup.[123] Further, some studies showed that the coalescence rate decreased with increasing pressure[124] and the initial bubble sizes near the gas distributor decreased at elevated pressure,[125] both of which are favorable to decrease the bubble size and increase the gas holdup.

3.4.4. Influence of Temperature. With an increase in the temperature, the liquid viscosity and surface tension decrease and result in a smaller average bubble size and a narrower bubble size distribution. Saxena et al.[77] investigated the bubble columns with gas−liquid and gas−liquid−solid systems within a 297−343 K temperature range and found a temperature dependence of the gas holdup only in the two-phase system. Soong et al.[126] found that the Sauter mean bubble diameter remarkably decreased with increasing temperature at a constant superficial gas velocity in a gas−liquid−solid slurry system. Lin et al.[71] found that, for a fixed pressure and superficial gas velocity, the increasing temperature generally increased the gas holdup but this influence was rather complex. Pohorecki et al.[127] found a decrease in the bubble swarm velocity and an increase in the gas holdup with increasing temperature. Schäfer et al.[128] experimentally studied the influences of the gas density, surface tension, liquid viscosity, gas distributor, and operating conditions on the bubble size. They reported that the stable bubble size decreased with a decrease in the liquid viscosity or surface tension and increasing temperatures resulted in reduced bubble size. Lau et al.[129] found that the influence of the temperature is generally not very notable and this temperature influence is more significant in high pressures than in low pressures.

3.4.5. Influence of Solid Concentration. To increase the reactor capacity and catalyst loading, the slurry reactor should be operated in high solid concentrations. However, the increase of solid concentration may have a negative influence on the hydrodynamics and gas−liquid mass transfer. It is therefore important to identify practical operational limits and the design implications of increasing solid concentrations in the column. For example, the gas distributor design and column startup procedure could be influenced by high solid concentrations.[18]

3.4.5.1. Influence of α_s on the Viscosity of Liquid−Solid Suspensions. In a gas−liquid−solid slurry system, the particles are usually smaller than 100 μm. In such cases, the spatial profile of the solid concentration is almost uniform. The main influence of the solid concentration lies in an increase in the apparent viscosity. Actually, the influence of increasing liquid viscosity and solid concentration on the hydrodynamics is qualitatively similar,[80,83,130] as shown in Figures 11 and 12.

The liquid−solid suspension can be divided into completely a dispersed suspension and coagulated suspension. The influence factors include the particle size distribution, solid surface characteristics, solid−liquid interaction, and flow shear rate. The completely dispersed suspension is relatively simple, in which the influence of the solid concentration on the apparent viscosity can be described by Einstein's theory, $\eta_{sus}/\eta_l = 1 + 2.5\alpha_s$, for the well-dispersed dilute suspension with uniform spherical particles, and by many other extended models[131,132] and empirical correlations[133−135] for a wider solid concentration range. The typical influence of the solid concentration on the apparent viscosity of a completely dispersed suspension is shown in Figure 13.[136] For a coagulated suspension, the apparent viscosity complexly depends on the flow shear rate, solid surface characteristics, and solid−liquid interaction. Particle coagulation

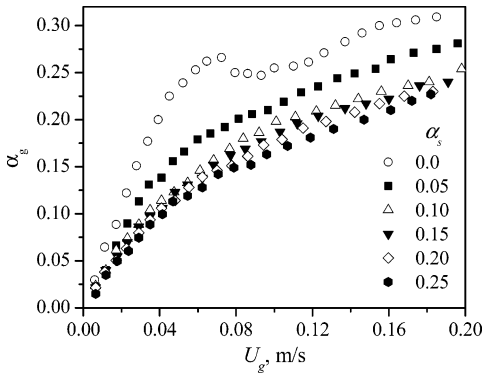

Figure 12. Influence of solid concentration on gas holdup reprinted with permission from the work of Vandu et al.[80] Copyright 2004 John Wiley & Sons, Ltd.

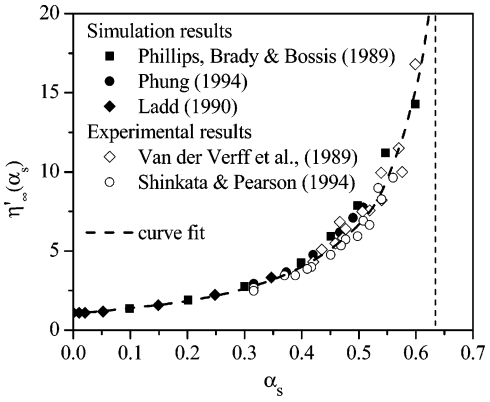

Figure 13. Influence of solid volume fraction on suspension dynamic viscosity reprinted with permission from the work of Brady.[136] Copyright 2001 Elsevier Limited.

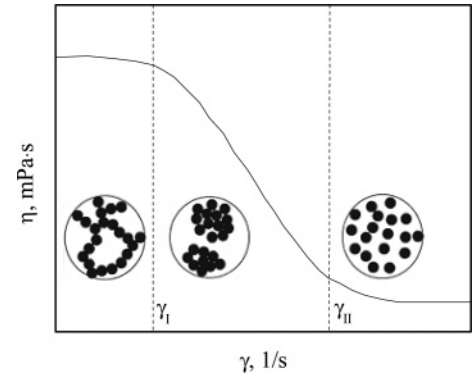

Figure 14. Influence of particle coagulation and shear rate on the dynamic viscosity of suspension: (1) Percolating network; (2) dispersed suspension; (3) suspension of clusters (reprinted with permission from the work of Perez et al.[138] Copyright 2000 Elsevier Limited).

commonly exists in a suspension with fine particles of nanoscale but also in some suspensions of micrometer-sized particles with special solid surface characteristics and liquid−solid interaction. For example, using a silica particle of 1.62 μm as the solid phase, Usui[137] prepared a completely dispersed suspension using ethylene glycol with 0.005 mol/L KCl as the solvent and prepared an agglomerative suspension using distilled water with 0.01 mol/L KCl as the dispersing media. The rheology of a coagulated suspension is much more complex than that of a dispersed suspension, as shown in Figure 14.[138] At high shear rates, the particles are completely dispersed. Below a given value of $\dot{\gamma}_s$, an increase in the apparent viscosity is observed resulting from an increase in the effective volume fraction, which includes the volume of both solid and entrapped liquid.

Although the particles in a slurry reactor are commonly 10−100 μm that are much larger than particles in a colloid system, the coagulation phenomenon still exists to some extent in such systems because: (1) very fine particles will be produced due to particle attrition;[139] (2) coagulation may occur for relatively coarse particles of ~10 μm when the particle−particle surface interaction is strong. This may explain the results of Li et al.[27] that gas holdups in suspensions of 11 μm particles were slightly lower than in suspensions of larger particles (35 and 93 μm) in the same solid volume fraction.

3.4.5.2. Influence of α_s on Bubble Behaviors. Increasing solid concentration generally increases the bubble size.[53,140] This was attributed to an increase in the apparent suspension viscosity with increasing solid concentration. At high solid concentrations, the bubble coalescence tendency is enhanced so that the fraction of small bubbles becomes insignificant.[71] Bubble breakup that occurs above the gas distributor is suppressed in the presence of fine particles in the suspension.[18] Prakash et al.[141] utilized yeast cells in a bubble column and reported that, as the yeast concentration increased, the rise velocity of large bubbles increased, whereas the rise velocity of small bubbles decreased. Behkish et al.[19] found that the volume fraction of small bubbles strongly decreased with increasing solid concentration in the gas−liquid−solid slurry system.

3.4.5.3. Influence of α_s on Gas Holdup. An increasing solid concentration generally decreases the gas holdup.[18,72,130,142] Although a bubble of the same size has a smaller rise velocity in a system with higher solid concentration,[140] the significant increase of the average bubble size with increasing solid concentration results in an increase in the bubble rise velocity and a decrease in the gas holdup. The decrease of the gas holdup with an increasing solid concentration is primarily due to the reduction in the holdup of small bubbles.[52] With an increase in the solid concentration, the transition superficial gas velocity decreases, and the operation range in the homogeneous regime becomes progressively narrower. The decrease of the gas holdup with increasing solid concentration is more significant in low solid concentrations than in high solid concentrations. Kara et al.[143] found that the decrease of the gas holdup is more significant from 0 to 25 wt % than at higher catalyst concentrations. Luo et al.[72] also found that the decrease of the gas holdup is more notable when the solid volume fraction increases from 0 to 0.081 than that from 0.081 to 0.191. Similar results were obtained by Inga and Morsi,[142] Gandhi et al.,[18] and Li et al.[27]

The influence of the solid concentration shows different characteristics in different superficial gas velocity ranges. Kato et al.[144] reported that the influence of the solid concentration on the gas holdup is more significant at superficial gas velocities higher than 10 cm/s. Similar results were obtained by Gandhi et al.[18] Also, the influence of the solid concentration on the gas holdup shows different characteristics in different pressure ranges. Luo et al.[72] found that, at ambient pressure, the gas holdup in the bubble column was almost 100% higher than in the slurry with solid volume fraction of 0.191 in the entire superficial gas velocity range; in contrast, at the pressure of 5.6 MPa, the influence of the solid concentration on the gas holdup was relatively small in superficial gas velocities above 25 cm/s.

3.4.6. Influence of the Gas Distributor. The gas distributor is an important factor that affects the bubble characteristics, which, in turn, affect the gas holdup, mass transfer, and other parameters. Commonly used gas distributors include the perforated plate, porous plate, membrane, porous tubes, and ring type and arm type distributors. In the porous type gas distributors, the pores in the plate or tubes are large enough for adequate passage of gas but small enough to prevent solid particles from entering the pores. However, significant clogging of pores may occur, e.g., due to solid particle attrition or failure of the gas feed supply. Furthermore, the relatively small pores cause high-pressure drops across the pores. Problems associated with ring type or arm type distributors include the danger of drainage of liquid−solid suspension into the gas supply system in the case of failure of the gas feed supply. This danger exists when the gas outlets are situated above or at the same level as the gas supply system. To solve these problems, Boer and Schrauwen[145] disclosed a gas distributor that comprises a feed pipe arrangement for feeding reactants to the spargers on the floor of the reactor, via a distribution system disposed above the spargers. The outlets of the spargers were typically oriented toward the floor or parallel to it in order to eject gas across the floor. This reduced settling of catalyst on the floor of the reactor, which improved mixing of the slurry and reduced the problems associated with uncontrolled reactions. For reactor scale-up, Coppens[146] disclosed a gas sparger consisting of pipes or channels that were connected in a hierarchical fashion so that the fluid entering the first channel was divided into channels of the same or different diameter and length, each or some of which were further divided into channels of the same or different diameter and length, and so on. The gas sparger could also consist of combinations of such treelike or fractal-like elements, embedded in the plane or in space. Such designs could have a good performance for reactors in a large scale.

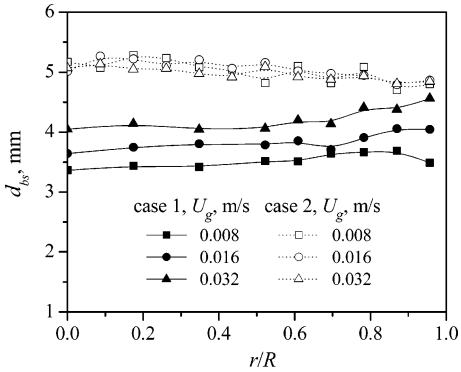

Figure 15. Influence of gas distribution on bubble size reprinted with permission from the work of Lin et al.[94] (Copyright 2004 Elsevier Limited): (case 1) porous sinter plate; (case 2) perforated plate.

In the gas distributor, small orifices enable the formation of smaller bubbles. Schumpe and Grund[81] worked with the perforated plate and ring type gas distributor and concluded that, with the ring type distributor, gas holdups of both small and large bubbles were smaller compared those with the perforated plate and the small bubble holdup showed a gradual increase with increasing superficial gas velocity. Bouaifi et al.[147] stated that, the smaller the bubbles, the greater the gas holdup values. Thus, they concluded that the gas holdup values were higher with a small orifice gas distributor. Lin et al.[94] studied the influence of different gas distributors, i.e., porous sinter plate (case 1) and perforated plate (case 2), in an external-loop airlift reactor. Figure 15 compares the bubble sizes in the two cases. The bubble sizes are much smaller in case 1 than in case 2, showing that the porous sinter plate has a better distribution performance. Their results also show that the radial profile of the gas holdup in case 1 is much more uniform than that in case 2 in the studied superficial gas velocity range. Zahradník et al.[83] studied the influence of the gas distributor and found significant influences of the gas distributor on both formation of the homogeneous regime and the values of the gas holdup,

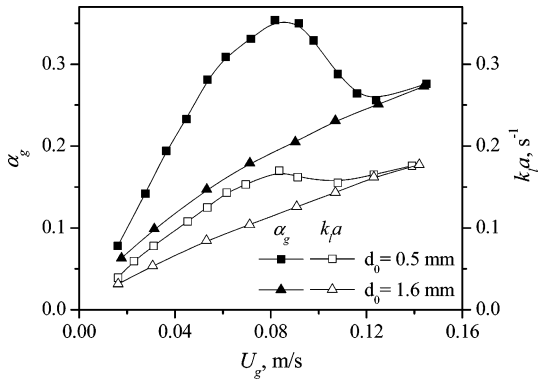

Figure 16. Influence of gas distribution on gas holdup and volumetric mass transfer coefficient reprinted with permission from the work of Zahradník et al.[83] Copyright 1997 Elsevier Limited.

as shown in Figure 16. With the perforated plate, the gas holdup with respect to the superficial gas velocity exhibited pronounced maxima for orifices of 0.5 mm; while for orifices larger than 1.6 mm, the homogeneous regime cannot be generated. The results also showed that the gas holdup was independent of the orifice diameter in the heterogeneous regime. The industrial slurry reactor for gas-to-liquid processes is usually operated in relatively high superficial gas velocities and solid concentrations and, thus, in the typical heterogeneous regime. In such cases, the ring type distributor and arm type distributor are recommended to give a good performance on block resistance.[145,148] While for gas−liquid processes operated in low superficial gas velocities, gas distributors with higher efficiency, such as the porous plate, membrane, or perforated plate with small orifices, are preferred.

3.4.7. Influence of Reactor Dimensions. 3.4.7.1. Influence of Reactor Dimensions on Gas Holdup. The knowledge of the influence of reactor dimensions on the gas holdup is vital for the scale-up and design of industrial reactors. The column dimensions are usually expressed by column diameter D, height H, and aspect ratio H/D.[50] It is commonly accepted that the hydrodynamics are independent of the column size, if D, H, and H/D are larger than some minimum values. Different minimum values have been reported. For example, the diameter D should exceed 0.1−0.2 m,[83,149,150] the height H should be larger than 0.3−0.5 m[151] or even 1−3 m,[150] and the aspect ratio H/D should be larger than 5.[83,150,152−154]

On the basis of the above discussion, for industrial reactors several meters in diameter, the column diameter will have negligible influence on the average gas holdup. It should be pointed out that when using experimental results obtained in a laboratory reactor apparatus to design an industrial reactor, the laboratory apparatus muse have a diameter larger than the critical value, say 0.15 m. In a bubble column with smaller geometrical parameters, the gas holdup decreases with an increase in D,[83,129,155] H,[150,156,157] or H/D.[153,154] Zhu et al.[158] measured the gas holdup in different axial positions and found that the gas holdup near the gas distributor was much higher than the average gas holdup. Urseanu et al.[102] studied the gas holdup in bubble columns of 0.15 and 0.23 m and found that the gas holdup decreased with increasing column size for liquids of both low and high viscosities. The decrease of the gas holdup with increasing H was explained by the three-region concept:[150,159] the bottom and top regions had higher gas holdup than the middle region, and the relative influence of the end regions decreased with increasing H where the middle region with relatively low gas holdup dominated. It should be mentioned that although the decrease of the gas holdup with increasing D was reported by the vast majority of investigators, the opposite trend was also indicated for narrow columns.[150,152]

3.4.7.2. Influence of Reactor Dimensions on Liquid Velocity. The column diameter has a significant influence on the radial profile of the liquid velocity. Forret et al.[160] found that, at the superficial gas velocity of 0.15 m/s, the centerline liquid velocity increased from 0.44 m/s in a column of 0.15 m to 1.04 m/s in a column of 1.0 m. Similar profiles of u_l/u_{l0} were obtained independent of the column diameter up to 1.0 m. Therefore, the knowledge of the centerline liquid velocity, u_{l0}, was enough to describe the whole liquid circulation. This was also confirmed by Krishna et al.[100] and Wu and Al-Dahhan.[95]

3.5. Mass Transfer. The mass transfer rate was described as the volumetric mass transfer coefficient. The liquid−solid mass transfer coefficient is on the order of magnitude of 10^{-4} m/s,[161] which is comparable to the gas−liquid mass transfer coefficient.[162] However, the liquid−solid interfacial area is much larger than the gas−liquid interfacial area at the same gas holdup and solid holdup, because the particle sizes in a slurry system are much smaller than bubble sizes. Thus, the resistance of liquid−solid mass transfer is negligible compared with the gas−liquid mass transfer, and only the latter one will be discussed below.

3.5.1. Similarity of Mass Transfer and Gas Holdup. In general, the variation of the volumetric mass transfer coefficient, $k_l a$, is similar to that of the gas holdup with respect to the superficial gas velocity, liquid viscosity, solid concentration, pressure, and temperature. In the literature, some correlations related $k_l a$ directly to the gas holdup instead of operating parameters and predicted $k_l a$ from the gas holdup data to the power of 1−1.18.[78,117,121,130,149,163] Letzel et al.[117] found that the ratio $k_l a/\alpha_g$ in the nitrogen−water system was almost constant and had a value of approximately 0.5 1/s at varying system pressures. Jordan and Schumpe[119] also found that $k_l a/\alpha_g$ in the nitrogen−decalin system was almost independent of the superficial gas velocity and gas density and has a value of about 0.45 1/s. Vandu and Krishna[130] measured the volumetric mass transfer coefficient for the air−water system in bubble columns of different diameters, 0.1, 0.15, and 0.38 m, with the superficial gas velocity in the range of 0 to 0.35 m/s. For superficial gas velocities above 0.08 m/s, the value of $k_l a/\alpha_g$ was found about 0.48 1/s, practically independent of the column diameter and superficial gas velocity.

Vandu and Krishna[130] investigated the volumetric mass transfer coefficients in gas−liquid systems with different liquids (water, tetradecane, paraffin oil, and Tellus oil with viscosities ranging from 1 to 75 mPa•s) and found that $k_l a/\alpha_g$ in the churn-turbulent regime shows a $Sc^{-1/3}$ dependence, where Sc is the Schmidt number of the liquid phase. They also found that $k_l a/\alpha_g$ significantly decreased with increasing solid concentration, which resulted from larger bubble sizes caused by enhanced bubble coalescence. However, Vandu et al.[121] found an increase in $k_l a/\alpha_g$ with increasing solid concentration (gas phase air; liquid phase C_9−C_{11} n-paraffin mixture; solid phase Sasol PURALOX ScCa 5/170, an alumina-based catalyst particle carrier). Chaumat et al.[164] plotted $k_l a/\alpha_g$ as a function of the superficial gas velocity and found the values of $k_l a/\alpha_g$ varied from 0.12 to 0.23 1/s, much lower than those obtained by Vandu and Krishna.[130] In addition, this ratio was not a constant even in the heterogeneous regime: it increased with increasing superficial liquid velocity. The authors claimed that the relationship between α_g and $k_l a$ appeared to be more complex than the oversimplified direct proportion. Nevertheless, the literature survey indicates that the superficial gas velocity, pressure, and

column diameter have insignificant influence on $k_l a/\alpha_g$, thus $k_l a/\alpha_g$ provides a useful scale-up rule, although not strict, for estimating $k_l a$ for industrial reactors of large diameter and operated at high superficial gas velocities and pressures.

3.5.2. Influence of Superficial Gas and Liquid Velocities. The superficial gas velocity is the dominant factor that influences $k_l a$. With increasing superficial gas velocity, $k_l a$ increases, less pronounced in the heterogeneous regime than in the homogeneous regime.[19,117−119,121,129,164−166] Tang and Fan[167] found that increasing the liquid velocity significantly increased $k_l a$ but only slightly increased the gas holdup. Yang et al.[165,166] and Chaumat et al.[164] found a slight increase in $k_l a$ with increasing superficial liquid velocity. The enhancement of mass transfer at higher liquid velocities is probably due to the turbulence induced by the liquid flow. Lau et al.[129] found that the influence of the liquid velocity on $k_l a$ became more pronounced at high pressures. For example, at 2.86 MPa, increasing the liquid velocity from 0.17 to 0.26 cm/s increased the mass transfer coefficient by as much as 30%.

3.5.3. Influence of Pressure and Temperature. The gas holdup and volumetric mass transfer coefficient increase with increasing pressure[19,117,129,168−171] or gas molecular weight.[172,173] Kojima et al.[169] found that both the gas holdup and volumetric mass transfer coefficient increased with increasing pressure and, for the single-nozzle gas distributor, the influence of the pressure on the gas holdup and volumetric mass transfer coefficient became significant at higher superficial gas liquid viscosities. Ozturk et al.[172] studied the mass transfer behavior in various organic liquids and found that the volumetric mass transfer coefficient increased with increasing gas density. The influence of temperature on the gas−liquid mass transfer is much more notable than on the gas holdup, due to the higher liquid diffusivity at high temperatures. Jordan and Schumpe[119] found that increasing temperature had little influence on the gas holdups in ethanol and decalin but increased the mass transfer coefficients, mainly, by higher oxygen diffusivity. Lau et al.[129] found that $k_l a$ increases from 0.03 to 0.17 1/s when the temperature increases from 25 to 92 °C. As for the corresponding gas holdup, it only increases from 0.24 to 0.30.

3.5.4. Influence of Solid Concentration and Liquid Viscosity. Most results in the literature show that the volumetric mass transfer coefficient decreases with increasing solid concentration[19,130,149,173,174] or liquid viscosity.[118,173,175,176] However, different results were also reported. Vandu et al.[121] found that the volumetric mass transfer coefficient was virtually independent of the solid concentration for the C_9-C_{11} paraffin oil slurries with Sasol PURALOX ScCa 5/170 (an alumina-based catalyst particle carrier) as the solid phase. The authors concluded that the natures of the solid particles and of the liquid phase were important determinants on the variation of the volumetric mass transfer coefficient with the solid concentration. In some systems, the volumetric mass transfer coefficient has a maximum value in the low-solid-concentration range.[165,166,177−179] The possible explanation for this is that, in the range of low solid concentration, the existence and movement of particles take the effects of breaking bubbles and enhancing the turbulence of the liquid phase, which are favorable to intensify the gas−liquid mass transfer. In the range of high solid concentration, the increased solid concentration results in an increase in the apparent suspension viscosity and a decrease in the gas−liquid mass transfer rate.

3.5.5. Influence of Surfactants. The presence of surfactants affects the bubble generation process, hence the specific interfacial area, liquid-side mass transfer coefficient, and volumetric mass transfer coefficient. The influence of surfactants on the gas and liquid mass transfer was rather complex, and different results were reported in the literature. Muller and Davidson[180] experimentally studied the effect of surface active agents on the mass transfer with viscous media and reported that the presence of octanol in solution increased the volumetric mass transfer coefficient $k_l a$ by 50%. The authors attributed this increase to the creation of small bubbles and reduced bubble coalescence due to surfactants. In contrast, different results were reported by some other authors that both $k_l a$ and k_l values markedly decreased with the presence of surfactants.[181−185] Vázquez et al.[182] found a reduction in the interfacial area with the addition of surfactant; however, Painmanakul et al.,[183] Azher et al.,[184] and Sardeing et al.[185] found that the interfacial areas in surfactant solutions were significantly larger than those in water. Sardeing et al.[185] found that the presence of surfactants decreased the bubble diameters, and they described three zones on the variation of the liquid-side mass transfer coefficient with the bubble diameter: for bubble diameters less than 1.5 mm, the k_l values are roughly constant at 1×10^{-4} m/s and no effect of the surfactants was observed; for bubble diameters greater than 3.5 mm, the k_l values were nearly constant with the bubble diameter but depended on the surfactant concentration; for bubble diameters between 1.5 and 3.5 mm, the k_l values increased from 1×10^{-4} m/s to the value reached at 3.5 mm and also depended on the surfactant concentration.

3.5.6. Mass Transfer Coefficient and Interfacial Area. Most studies on the mass transfer behavior are limited to determining the volumetric mass transfer coefficient, $k_l a$. Unfortunately, $k_l a$ is global and not sufficient to provide a better understanding of the mass transfer mechanism. The separation of k_l and a allows to identify which one of k_l and a controls the mass transfer.[147,166,170]

Wilkinson et al.[168] found that both $k_l a$ and a increased with increasing pressure in a 0.158 m bubble column using a ring gas distributor with 19 holes of 10 mm. Behkish et al.[147] suggested that the gas−liquid mass transfer in the heterogeneous flow regime and high solid concentrations were controlled by the gas−liquid interfacial area. Stegeman et al.[186] studied the influence of the superficial gas velocity, pressure, and liquid viscosity on the gas holdup and gas−liquid interfacial area in a bubble column. The reactor was operated at pressures between 0.1 and 6.6 MPa, and the gas distributor was a perforated plate with 284 holes of 0.4 mm. The liquid viscosity was varied in the range from 1.0 to 9.4 mPa·s. Their results showed that the pressure had a small influence on the gas holdup in pure water but had a pronounced influence on the gas holdup for more viscous liquids. For the most viscous liquid, all interfacial area data were obtained in the fully heterogeneous regime and it was demonstrated that the interfacial area increased with increasing pressure and was moderately affected by the superficial gas velocity. For the less viscous liquids, both the pressure and superficial gas velocity affected the interfacial area and this influence depended on the flow regime. Stegeman et al.[186] concluded that the flow regime had an important influence on the mode in which the operating parameters affected the interfacial area. Pohorecki et al.[187] studied the influences of the temperature and pressure on the bubble size and gas holdup for the nitrogen−water system in a temperature range of 30−160 °C and a pressure range of 0.1−1.1 MPa. The column was equipped with several gas distributors of different geometries. The bubble sizes were found to be independent of the position in the column, distributor geometry, superficial gas velocity, temperature, and pressure. The gas holdup was found to be

dependent only on the gas superficial velocity. The values of the interfacial area, calculated from the experimental values of the bubble size and gas holdup, were also found to be dependent only on the gas velocity. Maalej et al.[162] found that, for a given superficial gas velocity, both $k_l a$ and a increased, while k_l remained constant whatever the operating pressure; for a fixed gas mass flow rate, both $k_l a$ and a decrease with increasing operating pressure. Yang et al.[166] found that both the interfacial area and mass transfer coefficient increased with increasing superficial gas and liquid velocities. They also found that k_l increased greatly with increasing solid concentration in the low-solid-concentration range and decreased slowly with a further increase in solid holdup. Vandu et al.[121] found that k_l for large bubbles was practically independent of the superficial gas velocity and had values in the range of 0.002−0.003 m/s, about 1 order of magnitude higher than those estimated from the correlation proposed by Akita and Yoshida.[78] This higher k_l value can be attributed to the frequent bubble breakup and coalescence of large bubbles, which enhance the renewal of the gas−liquid interface. Lemoine[115] studied the hydrodynamic and mass transfer characteristics in organic liquid mixtures in a large-scale bubble column for the toluene oxidation process. They found that both k_l and a increased with increasing superficial gas velocity. Increasing pressure, on the other hand, increased both $k_l a$ and a but decreased k_l.

3.6. Liquid−Solid Separation. In FT synthesis in a slurry reactor, it is necessary to maintain the slurry at a constant level, removing the liquid products from the reactor. One problem with the removal of liquids, however, is that catalyst particles are dispersed in the liquid and must be separated from the slurry and, in some cases, returned to the reactor in order to maintain a constant inventory of catalyst in the reactor. Both iron catalyst and cobalt catalyst are currently used for FT synthesis. Separation of wax from supported cobalt catalysts is much easier than for unsupported iron catalysts due to attrition resistance of the support material.[11] The unsupported iron catalyst will be rapidly broken down to produce fine particles of 1−3 μm,[188] which further increases the difficulty of the liquid−solid separation, for example, blinds the pore openings of the filter. To solve problems with solid separation from the liquid products, Sasol paid attention both to physical characteristics of the catalyst and the separation processes themselves. Several techniques were evaluated; these findings were considered to be proprietary information. Stringent specifications for solids in the final wax cut were claimed to have been easily met.[17]

In general, there are two types of liquid−solid separators: in-reactor separators and external separators. A comprehensive review of the liquid−solid separation for the FT synthesis process was given by Zhou and Srivastava,[189] in which the liquid−solid separation approaches were divided into filtration, settling, centrifugation, vacuum distillation plus thermal cracking, high gradient magnetic separation, and chemical conversion. It was concluded that gravity settling, centrifugation, pressure filtration, and high gradient magnetic separation were technically feasible, either singly or in combination. In this section, recent developments on the liquid−solid separation for a slurry system will be reviewed.

3.6.1. Settling Method. Gravity settling is a commonly used, simple, and inexpensive method for FT wax−catalyst separation, but a long settling time of 1−3 h is required to reduce the solids content in the wax to 0.1 wt %. Zhou and Srivastava[189] reported that the British Greenwich FT pilot plant operated a gravity settling system fairly well. Mobil utilized an external system in which slurry was circulated by density differences and the time in the separator was sufficient for the slurry to settle so that solids-rich and nearly solids-free zones were formed. It may be difficult to achieve very low solids content, e.g., 1−2 ppm, for the wax by means of settlers and hydroclones. However, they can be a good preliminary separation step to recover most of the catalyst particles from the slurry in the form of a concentrated catalyst underflow for recycling back to the reactor. The clarified wax overflow can subsequently be processed by more efficient but usually expensive techniques, such as pressure filtration and magnetic separation to required low solid content.

Benham et al.[190] disclosed a dynamic settler apparatus for wax−catalyst separation. The settler has a sealed chamber into which a vertical feed conduit extends downward for a substantial length so as to form an annular region between the inner walls of the chamber and the feed conduit. As the slurry flows into the annular region at the bottom of the settler, the heavier catalyst particles are carried down, removed from the settler at the bottom, and then recycled back to the reactor. The wax rises up in the annular region, and this clarified wax is removed at the top. In this dynamic settler apparatus, both gravity and the jet momentum cause the particles to move downward. The outlet pipe for clarified wax can optionally have a filter to further purify the wax. Both internal and external dynamic settlers can be used in series to further improve the wax−catalyst separation efficiency.

Hydroclones have been successfully employed for the liquid−solid separation in the petroleum refining industry and, recently, have been used in the FT synthesis process. Clerici and Belmonte[191] disclosed using hydroclones coupled with a porous filter for the liquid−solid separation for the FT synthesis process. The hydrocyclone separates the suspension into the underflow concentrated in solids and the overflow diluted in solids. The diluted overflow is further separated by the micro-/ultrafiltration element to give the liquid product.

3.6.2. Filtration Method. Rytter et al.[192] described a vertical cylindrical filter in the form of a fine meshed screen located inside the reactor within the slurry. In the examples, models were used for the separation rather than a working reactor. Sasol described in some detail their operation in a large pilot plant with a slurry bubble column using a filter.[193] Anderson[194] disclosed a method in which the liquid product is separated from the catalyst particles by passing the liquid product through a plurality of cylindrical filters located within the reactor, such that the liquid passes through the filters and the catalyst particles conglomerate on the outside of the filters. As the liquid product is removed from the filters, a portion of it is pumped into a pulse surge vessel, such that the pressure of the pulse surge vessel is higher than the pressure of the FT reactor. At the time that it is desirable to remove the conglomerated catalyst on the filters, the liquid product through the filters is stopped and a high-pressure liquid product is sent from the pulse surge vessel to a back-flushing liquid inlet of the filter to dislodge the conglomerated catalyst particles. Müller[195] reported using the FUNDABAC filter family for liquid−solid separation. In the FUNDABAC filtration system, each element is composed of six filter tubes that were arranged around a central filtrate tube. This created a so-called clover leaf pattern in cross section. This unusual design promoted good adherence of the filter cake to the filter cloth, i.e., the concave areas of the filter element caused the cake to adhere during compression and guaranteed that it remained in place throughout the entire cycle.

3.6.3. Other Liquid−Solid Separation Methods. 3.6.3.1. Extraction. The U.S. DOE patented a process that separates the catalyst from the wax product using a dense gas and/or liquid

extraction in which the organic compounds in the wax are dissolved and carried away from the insoluble inorganic catalyst particles.[196] When extraction is used in conjunction with magnetic field separation, the electromagnets are added to the interior and/or exterior of the separator. An additional separating step, such as fine particle filtering, can also be used to remove catalyst from wax product. Brioles et al.[197] studied the use of near-critical fluid extraction to remove wax product to provide a solids enriched stream to return to the reactor and showed that this approach was promising.

3.6.3.2. High-Gradient Magnetic Separation. Brennan et al.[198] patented a method that separates catalyst fines from the wax product by high-gradient magnetic separation. In this method, the wax passes through the magnetic field while the catalyst fines which are typically iron-based or cobalt-based are held by magnetized filter elements. The magnet structure is expensive, but the operation and maintenance costs are low. Zhou and Srivastava[189] considered that this technique had the potential to be used inside the slurry reactor, conceivably as a section of the slurry recycle line surrounded by an external electromagnet.

3.6.3.3. Combination Method. Each liquid−solid separation method has its advantages and disadvantages. To satisfy the requirement of a commercial FT synthesis process, it is usually necessary to combine more than one liquid−solid separation method. Clerici and Belmonte[191] disclosed a method in which the liquid−solid separation was complemented with combination of hydrocyclone and filtration. The hydrocyclone provides a preliminary separation that separates most of the catalyst particles from the slurry and recycles them back to the reactor. The clarified wax is subsequently separated by filtration to required low solid content for further processing. Espinoza et al.[199] patented a method in which the difficulty in wax−catalyst separation caused by catalyst attrition was solved by using a settling system coupled with a filtration system. The settling system continuously or intermittently removes catalyst subparticle fines from the slurry by way of a subparticle-rich stream, and the filtration system separates the slurry into a catalyst-rich stream and a catalyst-lean stream that supplies the wax products. Through this way, the overall concentration of catalyst fines in the slurry is reduced, thereby increasing the effectiveness and the life of a liquid−solid separation system.

3.7. Hydrodynamic and Mass Transfer in Slurry Airlift Reactors. Many published works on airlift reactors are available in the literature. Thus, the discussion here was limited to the special characteristics, which are closely related to the gas-to-liquid processes, of airlift reactors compared with bubble columns. The global liquid circulation in an airlift reactor has the following influences: first, it is favorable to homogenously suspend the catalyst particles, which makes it possible to operate the airlift reactor in low superficial gas velocities without solid sedimentation; second, it makes the gas holdup and mass transfer coefficient in the airlift reactor considerably lower than in a bubble column;[200−202] third, the variation of the gas holdup and volumetric mass transfer coefficient with the system properties and operating conditions, such as the superficial gas velocity, pressure and temperature, liquid viscosity, and solid concentration, is less pronounced in the airlift reactor than in the bubble column.[203,204] This is because when the gas holdup increases due to a variation in the operating conditions, e.g., an increase in the superficial gas velocity, the liquid circulation velocity also increases, which has a restraining influence on the increase of the gas holdup and volumetric mass transfer coefficient.

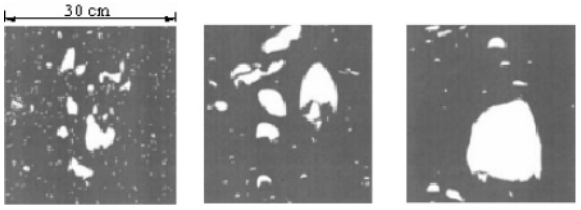

Figure 17. Influence of solid concentration on bubble size at the height of 0.65 m in a 2D column from reprinted with permission the work of de Swart et al.[70] Copyright 1996 Elsevier Limited.

In an airlift reactor, the gas holdup and liquid circulation velocity are the most important parameters, for which mathematical models have been proposed based on either momentum balance or energy balance.[69,204−207] In an airlift reactor, the liquid circulation velocity is determined by the balance between the flowing resistance and the driving force resulting from different gas holdups in the riser and downcomer. When the rector height is small, the flowing resistance in the bottom and top sections is the main part of the total resistance. With an increase in the reactor height, the proportion of the flowing resistance in the bottom and top sections decreases, and this, in turn, increases the liquid circulation velocity and decreases the gas holdup. Therefore, the liquid circulation velocity will be too high in a tall industrial airlift reactor. In such a case, it is necessary to install internals in the riser to decrease the liquid circulation velocity, increase the gas holdup, and enhance the gas−liquid mass transfer.

4. Process Intensification with Internals

4.1. Necessity of Using Internals. For high reactor productivity, the industrial slurry reactor needs to be operated at high superficial gas velocity and solid concentration. In the heterogeneous regime, the increase of the gas holdup with increasing superficial gas velocity slows down due to an increase in the large bubble fraction. With increasing solid concentration, the apparent viscosity of the slurry phase remarkably increases, which, in turn, increases the bubble size and decreases the gas holdup, as can be seen in Figure 17. In some systems, the gas-liquid mass transfer coefficient will decrease 3-fold when the solid volume fraction increases from 0 to 0.25.[130] Behkish et al.[19] reported that, at high solid concentrations, large bubbles were formed with enhanced bubble coalescence and they limited the mass transfer in the column. As a result, the authors concluded that, for industrial bubble columns, the presence of small bubbles should be preferred and the presence of large bubbles should be avoided for higher mass transfer rates. Dreher and Krishna[208] studied the influence of perforated plates on the liquid-phase back-mixing and found a reduction of the liquid-phase back-mixing in compartmentalized bubble columns.

The decrease of the gas holdup and increase of the bubble size have direct negative effects on the gas−liquid mass transfer, which, in turn, affects the conversion and productivity. A small initial bubble size can be achieved with an efficient gas distributor, but the effective region of the gas distributor is limited to only a certain height above the distributor, especially at high superficial gas velocities. Internals are effective to intensify the gas−liquid mass transfer, through the following mechanics: (1) decrease the bubble size and increase the gas holdup by increasing bubble breakup; (2) enhance the surface renewal by increasing liquid turbulence, bubble breakup, and bubble coalescence.

There is another important reason for using internals in the riser of an airlift reactor. In an airlift reactors, the liquid

circulation velocity increases with an increase in the reactor height or column diameter.[209] Thus, the liquid circulation velocity may be up to 2−3 m/s or even larger in a tall industrial airlift reactor. Internals have the function of controlling the liquid circulation to give larger gas holdup and mass transfer coefficients. Further, some of the kinetic energy of the flowing liquid is transformed into turbulent kinetic energy through the internals, which further enhances bubble breakup and gas−liquid surface renewal.

4.2. Influence of the Internals. In some works, the static mixer was used in the riser to improve the performance of mass transfer in an airlift reactor.[210−212] Lin et al.[211] observed that the oxygen mass transfer for the cultivation of a cell increased when a baffle-type static mixer was used. For non-Newtonian liquids, the advantages of the used static mixers on mass transfer were reported by Chisti et al.[210] and Stejskal and Potucek.[212] Okada et al.[175] examined the influence of a packed bed set in the riser on the volumetric mass transfer coefficient in an external-loop airlift reactor with water, 20 wt % glycerol, 10 wt % ethanol, and 0.3 wt % CMC aqueous solutions. The results showed that the presence of the packed bed in the riser increased the k_la values for all the liquids used. This increase in k_la was mainly associated with the increase in a due to bubble breakup by the packed bed. They also found that increasing the layer height of the packed bed was not an effective method for further decreasing the bubble size. Nikakhtari and Hill[213] inserted a small quantity of nylon mesh packing in the riser section of an external-loop airlift bioreactor and found that the overall volumetric oxygen mass transfer coefficient increased by a factor of 3.73 compared to an unpacked riser. The packing increased the gas holdup and decreased the bubble size and liquid circulation velocity, all of which contributed to the dramatic improvement in oxygen mass transfer.

For a slurry reactor, the internal used must be block-resistant while maintaining satisfactory performance of breaking bubbles. In such cases, internals with relatively simple structure may be of choice. Bendjaballah et al.[214] studied the influence of inserting a valve in the downcomer on the hydrodynamics in an external-loop airlift reactor and found that an increase in the flowing resistance by changing the valve opening resulted in a remarkable increase in the gas holdup and a delay in transition from the homogeneous to heterogeneous regime. Krichnavaruk and Pavasant[215] studied the influence of a perforated plate on the gas−liquid mass transfer in an airlift reactor, and found that the influence of the perforated plate was twofold. First, it helped in breaking large bubbles that passed through the plate. Second, the presence of a perforated plate seemed to lower the mass transfer coefficient. The former influence is dominant, with the gas−liquid interfacial area increasing to more than twice its original value. As a result, the overall gas−liquid mass transfer rate was enhanced with perforated plates inserted into the system. Wang et al.[69] studied the influence of the perforated plate on the overall gas holdup. The gas holdup in the riser with the perforated plate (case a) is about 2-fold that without a perforated plate (case b), as shown in Figure 18. Zhang et al.[216] studied the influence of a specially designed internal, called a *bubble scraper*, in an external-loop airlift reactor with the rise of 230 mm in diameter. The internal has been described in detail by Jin et al.,[76] and its structure is shown in Figure 19. This bubble scraper is 230 mm in diameter and 100 mm in height. The angle between the baffle of the internal and the vertical axis is 45°. Each baffle is 30 mm in width and 1 mm in thickness. There are some semicircular holes on the plate, and each hole has a tonguelike plate facing the upstream to break

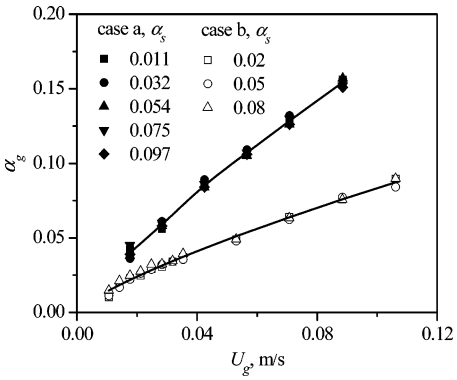

Figure 18. Influence of internals on the gas holdup in a air−water−solid slurry system. The data are from the work of Wang et al.[69]

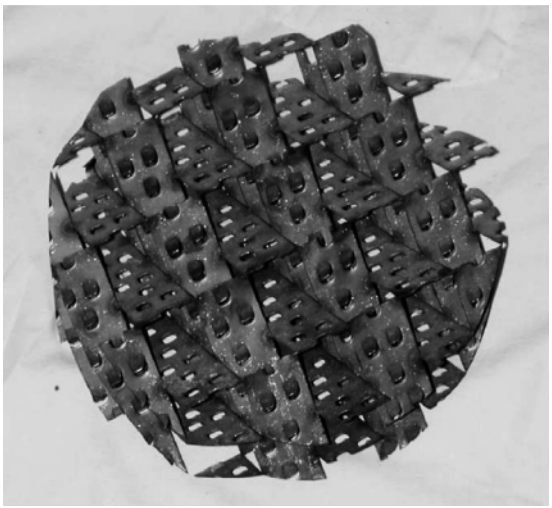

Figure 19. Photo of the internal bubble scraper reprinted with permission from the work of Zhang et al.[216] Copyright 2005 Elsevier Limited.

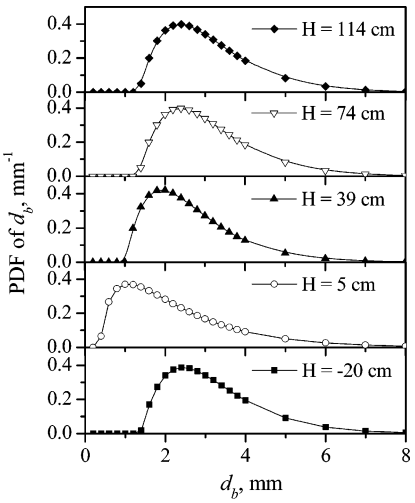

Figure 20. Influence of the bubble scraper on bubble size distribution in the air−water system. The data are from the work of Zhang et al.[216]

bubbles. The results showed that this internal had the remarkable effect of breaking bubbles, as shown in Figure 20, and made the radial profiles of the gas holdup and liquid velocity more uniform, as shown in Figure 21. The influences of the internal become insignificant with increasing distance after the internal. The effective distance was 1.0−1.5 m. Therefore, not only the structure of the internal but also the number of the internals and the distance between them should be optimized to give a better performance of intensifying the mass transfer and improving the hydrodynamics.

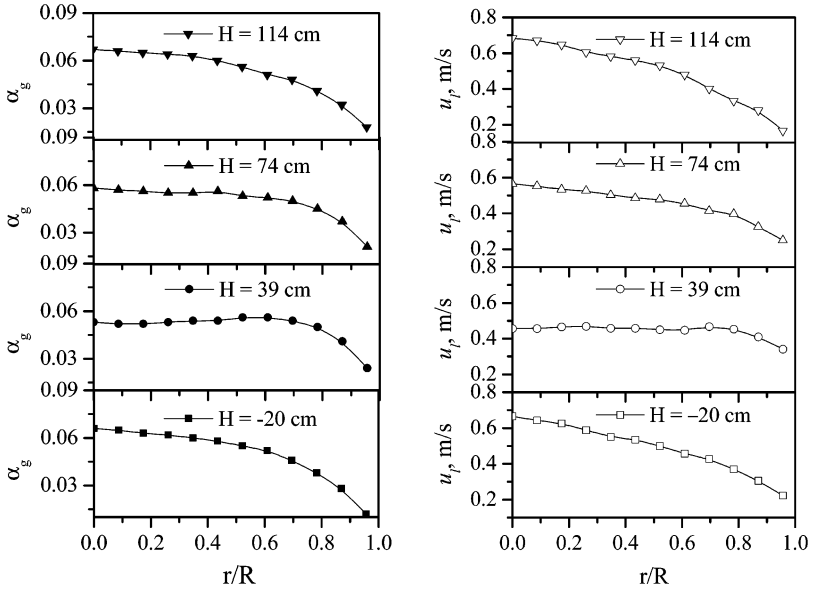

Figure 21. Influence of the bubble scraper on radial profiles of gas holdup and liquid velocity in the air−water system. The data are from the work of Zhang et al.[216]

Besides enhancing bubble breakup and improving the hydrodynamics, the internals also have the effects of decreasing the liquid back-mixing, which is desirable to approach high conversion.[208,217−219] Dreher and Krishna[208] found that installation of perforated sieve plates effectively restricted the liquid circulations between the compartments. Alvaréa and Al-Dahhanb[219] found that the compartmentalization of conventional bubble columns by perforated trays was very effective to reduce the liquid back-mixing. They studied the effect of tray design and operating conditions on the overall liquid back-mixing in a bench-scale trayed bubble column and found that a 3-fold reduction in the liquid back-mixing was achieved in the trayed column as compared to the column without the trays. Moreover, the tray open area and the superficial liquid velocity were found to have strong effects on the liquid back-mixing.

5. Modeling and Simulations

In order to develop design tools for engineering purposes, much research has been carried out in the area of computational fluid dynamics (CFD) modeling and simulation on gas−liquid and gas−liquid−solid flows. The particles used in slurry systems are fine and can be easily suspended in the liquid; therefore, the liquid and solid phases were usually treated as a pseudo-homogeneous phase.[84,220] The influence of the particles was taken into account by using the physical properties of the liquid−solid suspension, such as the density and viscosity. Two approaches are mostly used in the gas−liquid or gas−liquid−solid flows: the Euler−Lagrange approach[221,222] and Euler−Euler approach.[73,88,223,224] The Euler−Lagrange approach has the advantage of a clear physical description but the disadvantages of high computational cost and difficulties in considering bubble deformation, breakup, and coalescence. The Euler−Euler approach has the advantage that the model equations for each phase have the same form and the simulations need much less computations. Reactor-scale simulations usually use the Euler−Euler approach.

Several good reviews on modeling and simulation of the gas−liquid system were published in recent years.[15,225−227] In most CFD simulation works on dispersed gas−liquid and gas−liquid−solid flows in the literature, the local bubble size distribution was not used and a constant bubble size was used instead. This simplification limits such models to the homogeneous regime. In fact, it is very important to consider in detail the local bubble behavior for the following reasons:[74] (1) The bubble behavior has a significant influence on the flow regime transition, since the major phenomenon causing the transition from the homogeneous to heterogeneous regime is the occurrence of large bubbles. (2) The bubble size has a wide distribution in the heterogeneous regime, which is the usual case for an industrial reactor. (3) The complexity of bubble dynamics makes the radial profiles of the gas holdup and bubble rise velocity difficult to predict for a wide variety of conditions.[15,225] This is because the radial profile of the gas holdup is determined by the lateral forces, such as the transverse lift force, turbulent dispersion force, and wall lubrication force, and these lateral forces depend on the bubble size.[84,92,93,228] However, the lateral forces are ignored or simplified in most CFD simulations reported in the literature.[229−231] (4) Bubble breakup and coalescence have a significant influence on the interphase mass transfer.

Due to the importance of the bubble behavior, great efforts have been made to take into account the influence of the bubble size. Krishna et al.[91] proposed a so-called three-phase or two-class bubble model, in which the gas phase is divided into two classes of small and large bubbles. In recent years, more and more attention has been drawn to couple the PBM into the CFD framework. This concept was implemented as the so-called multiple-size-group (MUSIG) model in the commercial CFD package, CFX. However the bubble breakup and coalescence models used in CFX cannot give proper predictions in wide operating conditions. Several authors have made attempts to couple their own bubble breakup and coalescence models into the CFD framework. Chen et al.[75] used the population balance model with different bubble breakup and coalescence closures and concluded that the choice of bubble breakup and coalescence closure does not have a significant influence on the simulated results as long as the magnitude of breakup is increased 10-fold. This conclusion is not consistent with the results of Wang et al.,[63] where four typical bubble coalescence and breakup modes[48,58−60,62,73] were compared. The results show that the calculated bubble size distributions are quite different when different bubble coalescence and breakup models are used. The

bubble breakup and coalescence models are very important for proper prediction of the bubble size distributions in different flow regimes.

The two-fluid model with the assumption of constant bubble diameter can give reasonable predictions for the homogeneous regime because the bubble size distribution in such a condition is narrow and the bubble interaction is relatively weak. The most important issue of the CFD−PBM coupled model is therefore its ability of predicting the hydrodynamics in the heterogeneous regime where bimodal bubble size distributions are observed especially in high superficial gas velocities. However, most reported results by the CFD−PBM coupled model were either only for the homogeneous regime[232,233] or for both the homogeneous and heterogeneous regimes but did not successfully predict a bimodal bubble size distribution in the heterogeneous regime.[57,75] Exceptions are the results of Lehr et al.[73] and Wang et al.,[74] where the bimodal bubble size distributions were obtained. Lehr et al.[73] reported the 3D transient simulation results, in which the population balance was simplified to a balance equation for the average bubble volume. The gas phase was modeled as small and large bubble phases, and the small and large bubble fractions were calculated by the simplified balance equation. The bubble size was calculated with the assumption that the dimensionless number density distributions of the small and large bubble fractions are approximated by a lognormal distribution and an exponential distribution, respectively. Such simplification remarkably reduces the computation demands and makes the 3D transient simulations feasible. However, this simplification approach particularly depends on their bubble breakup and coalescence models and may be unfeasible for other models. The interphase drag force in their model was calculated with the Sauter mean diameter but not directly based on the bubble size distribution. Further, they neglected the wake effect of large bubbles on the interphase drag force, which is important in the heterogeneous regime.[88] The lateral forces were also neglected in their work. Experimental study and numerical simulations have proven that lateral forces are important for the formation of different radial profiles of the gas holdup,[84,92,93,234] as discussed earlier. Therefore, it is necessary to consider the lateral forces for correct prediction of different radial profiles of the gas holdup. All the reported simulations that neglect the lateral forces predict a flat or core-peaking radial profile of the gas holdup. These models cannot predict the wall-peaking radial profile of the gas holdup in a system with small bubbles.

Wang et al.[74] simulated the gas−liquid flow with a CFD−PBM coupled model. In that work, a full population balance model with detailed bubble breakup and coalescence models was coupled in the CFD framework. Different bubble breakup and coalescence models were compared. An algorithm was proposed to calculate the interphase forces and turbulence modification with a volume fraction averaged algorithm based on the bubble size distribution. The ability of the CFD−PBM coupled model to predict the hydrodynamics both in the homogeneous and heterogeneous regime was discussed in detail. The results showed that this CFD−PBM model had a good ability to predict the hydrodynamics both in the homogeneous and heterogeneous regimes and the different radial profiles of the gas holdup were also reasonably predicted, as shown in Figures 22 and 23. The CFD−PBM coupled model developed in this work has the following advantages: (1) it has the ability of both CFD to calculate the entire flow field and PBM to calculate the local bubble size distribution; (2) it combines the PBM into the CFD framework so that bubble breakup and coalescence can be taken into account and can describe the bubble size distribution in different flow regimes; (3) it takes into account the influence of the bubble size on the interphase interaction so that the CFD−PBM coupled model has the ability to predict the flow behavior in different flow regimes; (4) it predicts the local bubble size distribution and gas holdup from which the local gas−liquid interfacial area can be determined.

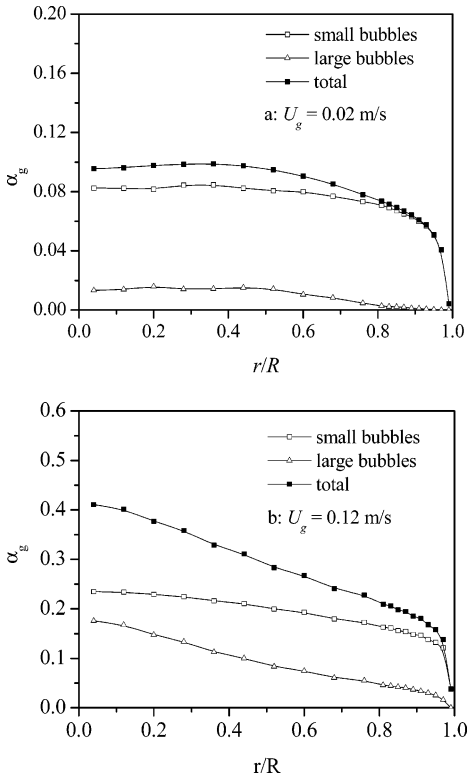

Figure 22. Radial profiles of gas holdups for small bubbles, large bubbles, and total bubbles predicted by the CFD−PBM coupled model reprinted with permission from the work of Wang et al.[74] (Copyright 2006 John Wiley & Sons, Ldt.). The parameters of the simulated column are as follows: ID = 0.19 m, H = 2.4 m. The results are for a height of 2.0 m.

Further study on the CFD−PBM coupled model will focus on quantitative description of the relationship between the gas−liquid mass transfer rate and bubble breakup and coalescence and the influences of pressure, liquid viscosity, and solid concentration on bubble behaviors.

6. DME Synthesis 3000 ton/year Pilot Plant

Fundamental research on the direct synthesis of DME from synthesis gas, including catalyst preparation and reactor and process development, was started in 1998 at the Department of Chemical Engineering, Tsinghua University, China. The development of a mass production technique for the direct synthesis of DME was started in 2002, cooperating with Chongqing Yingli Fuels & Chemicals Co. Ltd., and a pilot plant of 3000 ton/year was completed in 2004 in Chongqing. In this process, the syngas with the molar ratio of CO to H_2 of about 1, which was obtained using methane reforming with CO_2 and stream followed by removal of CO_2 and H_2, was compressed and fed into the slurry reactor filled with catalysts and inert liquid paraffin. After reaction, the effluent from the reactor is DME, byproduct CO_2, a small amount of methanol, and unreacted syngas. DME and other byproducts were absorbed with solvent and then purified, while the unreacted reactants in the vent gas were recycled.

The industrial experiments were carried out in three stages. The only difference between stages I and II is that the syngas

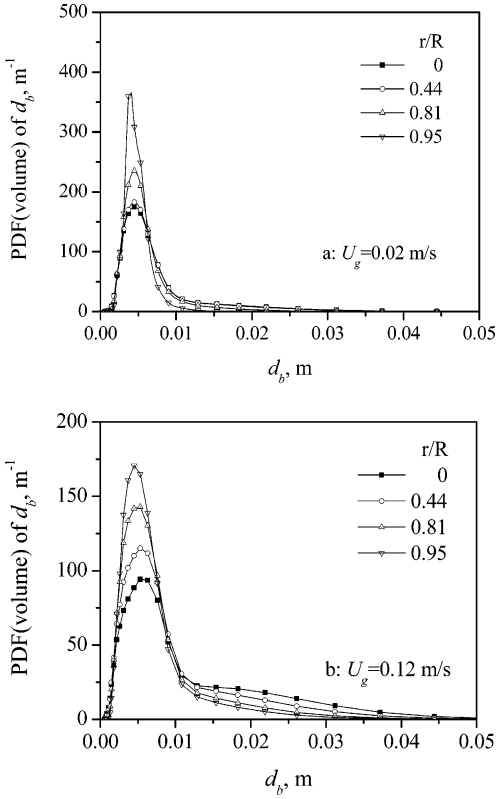

Figure 23. Bubble size distribution at different radial positions and different superficial gas velocities predicted by the CFD−PBM coupled model reprinted with permission from the work of Wang et al.[74] (Copyright 2006 John Wiley & Sons, Ldt.). The parameters are the same as those in Figure 20.

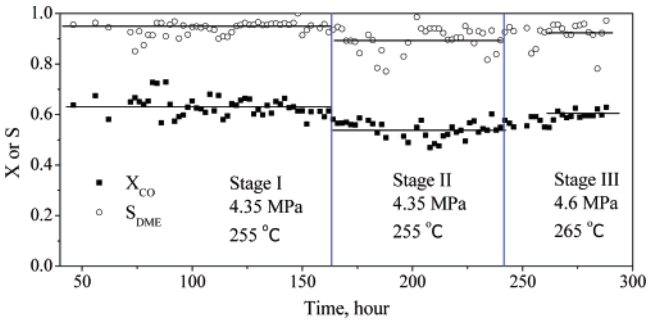

Figure 24. Conversion of CO and selectivity to DME in the pilot plant. The data are from the work of Ren et al.[9]

passes the slurry reactor without recycling the tail gas in stage I, while in stage II the tail gas was recycled. Compared with stage II, the temperature and pressure in stage III were promoted to increase the conversion of CO. Some of the conditions and results of the pilot plant are shown in Figure 24 and Table 1. It can be seen that in stage I the average once-through conversion of CO and selectivity to DME in the organic product can reach 63% and 95%, respectively. Because the tail gas was recycled in stage II, the high fraction of methane leads to a decrease in the average conversion of CO and selectivity to DME. In stage III, a little elevation of the reaction temperature and pressure can increase the average conversion of CO and selectivity to DME to 61% and 92%, respectively. These results are almost the same as those obtained in the laboratory, where a stirred autoclave reactor was used. It also proves that the slurry airlift reactor provides good performance on the mass and heat transfer in DME synthesis processes. Moreover, during the operation time, the catalysts showed no noticeable deactivation.

Table 2. Comparison of Pilot-Plant Results

conditions	JFE	Air Products	Tsinghua University
H_2/CO ratio	1	0.7	1
catalyst		Cu−Zn−Al+γ−Al_2O_3	LP201 + TH16
pressure (MPa)	5	5−10	4.35−4.6
temperature (°C)	260	250−280	255−265
CO conversion (%)	40	22	54−63
DME selectivity (%)	90	40−90	89−95
reactor type	slurry bubble column	slurry bubble column	slurry airlift reactor
diameter, height (m)	15, 0.55	15.2, 0.475	21.6, 0.6
design scale (ton/day)	5	10	10

Up to now, different processes for mass production of DME in a slurry reactor have been developed by Air Products,[8] JFE,[7] and Tsinghua University,[9] as shown in Table 1. In the above three processes, the catalysts are all composed of Cu-based materials for methanol synthesis and Al_2O_3 catalyst for methanol dehydration. The reactors used by JFE and Air Products are slurry bubble columns, while the reactor in the pilot plant in Chongqing is a slurry airlift reactor with internals. It can be found from Table 2 that the conversion of CO obtained in the slurry airlift reactor developed by Tsinghua University is obvious higher and the operation conditions are milder than the others.

7. Remarks and Conclusions

With the dramatic increase in the international oil price, gas-to-liquid processes, including FT synthesis, methanol synthesis, and DME synthesis, have become increasingly important. The slurry reactor has the advantages of simple construction, good heat transfer, and feasible scale-up, which make it very suitable for the gas-to-liquid processes. There has been an obvious shift in trends from the fixed bed reactor to the slurry reactor in the gas-to-liquid processes. The following remarks and conclusions can be drawn from this review:

(1) There are three types of slurry reactors, namely, the bubble column, airlift reactor, and spherical reactor. The slurry bubble column is the simplest in construction, while the other two reactor types have some special advantages. The slurry airlift reactor is favorable for homogeneously suspending the catalyst particles and, thus, has better operation flexibility. Further, the mass transfer can be greatly intensified by using internals in the riser, especially in the heterogeneous regime. The spherical reactor has economical feasibility and great potential for large-scale production in the fuel industry, since it has higher mechanical resistance to pressure than the cylindrical column, which decreases the wall thickness needed and the reactor cost.

(2) The hydrodynamic behavior, heat and mass transfer, and mixing behavior are quite different in the homogeneous and heterogeneous regimes. The current industrial interest in gas-to-liquid processes is the heterogeneous regime, which is much more complex than the homogeneous regime; however, the studies on this regime are still relatively limited. The GDG method and the two-bubble class model were widely used to study the heterogeneous regime. The population balance model developed quickly in recently years seems to be more promising for describing the complex bubble behaviors in the heterogeneous regime.

(3) The transition from the homogeneous to heterogeneous regime is delayed with increasing pressure and is advanced with

increasing solid concentration. Thus, the gas holdup and volumetric mass transfer coefficient increase with increasing pressure and decreasing solid concentration.

(4) For high reactor productivity, the industrial slurry reactor needs to be operated at high superficial gas velocity and solid concentration. In such cases, the mass transfer may become a rate-limiting step, and it is recommended to use internals to intensify the mass transfer and improve the hydrodynamics.

(5) Feasible liquid−solid separation methods include settling, filtration, and high-gradient magnetic separation. However, none of these approaches itself seems to achieve the requirement of a commercial FT synthesis process. It is recommended to use more than one liquid−solid separation method in combination, typically a settling separator followed by filtration or magnetic separation.

(6) Full CFD simulations become more and more important to obtain a better understanding of the complex hydrodynamics and mass transfer behavior. In the heterogeneous regime, the CFD−PBM coupled model which combines the population balance model into the computational fluid dynamics is an effective approach to describe the complex behaviors of bubble coalescence and breakup and bubble−bubble and bubble−liquid interactions. The mass transfer behavior and influences of the pressure, liquid viscosity, and solid concentration seem to be reasonably modeled in the framework of the CFD−PBM coupled model.

Acknowledgment

The authors gratefully acknowledge the financial support by the National Natural Science Foundation of China (No. 20576060 and No. 20606021), and the Foundation for the Author of National Excellent Doctoral Dissertation of PR China (No. 200757).

Nomenclature

a = gas−liquid interfacial area, m^{-2}
C_0, C_1 = parameters in the drift flux model, −
D = column diameter, m
d_0 = orifice diameter, m
H = column height, m
k_l = liquid-side mass transfer coefficient, m/s
N_c = dimensionless capacitance number of the chamber, defined as $4V_c g\rho_l/\pi d_0^2 P$
Sc = theliquid-phase Schmidt number, defined as $\mu_l/\rho_l D_l$
U_g = superficial gas velocity, m/s
u_l = local liquid velocity, m/s
U_l = superficial liquid velocity, m/s
u_{l0} = centerline liquid velocity, m/s
V_c = volume of gas chamber, m^3

Greek Letters

μ = viscosity, Pa·s
α_g = gas holdup
α_s = solid holdup

Literature Cited

(1) Krishna, R.; Sie, S. T. Design and Scale-up of the Fischer−Tropsch Bubble Column Slurry Reactor. *Fuel Process. Technol.* **2000**, *64*, 73.

(2) Wu, Y. X.; Gidaspow, D. Hydrodynamic Simulation of Methanol Synthesis in Gas−Liquid Slurry Bubble Column Reactors. *Chem. Eng. Sci.* **2000**, *55*, 573.

(3) Dry, M. E. High Quality Diesel via the Fischer−Tropsch Process − a Review. *J. Chem. Technol. Biotechnol.* **2001**, *77*, 43.

(4) Tijm, P. J. A.; Waller, F. J.; Brown, D. M. Methanol Technology Development for the New Millennium. *Appl. Catal. A: Gen.* **2001**, *221*, 275.

(5) Fleisch, T. H.; Sills, R. A.; Briscoe, M. D. 2002−Emergency of the Gas-to-Liquids Industry: a Review of Global GTL Developments. *J. Nat. Gas Chem.* **2002**, *11*, 1.

(6) Larson, E. D.; Ren, T. J. Synthetic Fuel Production by Indirect Coal Liquefaction. *Energy Sustainable Dev.* **2003**, *7*, 79.

(7) Ogawa, T.; Inoue, N.; Shikada, T.; Ohno, Y. Direct Dimethyl Ether Synthesis. *J. Nat. Gas Chem.* **2003**, *12*, 219.

(8) DOE/NETL−2004/1199, *Commercial-Scale Demonstration of the Liquid Phase Methanol (LPMEOHTM) Process, A DOE Assessment*; Department of Energy: Washington, D.C., 2003.

(9) Ren, F.; Wang, J. F.; Li, H. S. Direct Mass Production Technique of Dimethyl Ether from Synthesis Gas in a Circulating Slurry Bed Reactor. *Stud. Surf. Sci. Catal.* **2006**, *159*, 489.

(10) Frerich, J. K. Methanol-to-Hydrocarbons: Process Technology. *Microporous Mesoporous Mater.* **1999**, *29*, 49.

(11) Davis, B. H. Overview of Reactors for Liquid Phase Fischer−Tropsch Synthesis. *Catal. Today* **2002**, *71*, 249.

(12) Brown, D. M.; Bhatt, B. L.; Hsiung, T. H.; Lewnard, J. J.; Waller, F. J. Novel Technology for the Synthesis of Dimethyl Ether from Syngas. *Catal. Today* **1991**, *8*, 279.

(13) Lu, W. Z.; Teng, L. H.; Xiao, W. D. Simulation and Experiment Study of Dimethyl Ether Synthesis from Syngas in a Fluidized-Bed Reactor. *Chem. Eng. Sci.* **2004**, *59*, 5455.

(14) Longwell, J. P.; Rubin, E. S.; Wilson, J. Coal: Energy for the Future. *Prog. Energy Combust. Sci*. **1995**, *21*, 269.

(15) Joshi, J. B. Computational Flow Modeling and Design of Bubble Column Reactors. *Chem. Eng. Sci.* **2001**, *56*, 5893.

(16) Kantarcia, N.; Borakb, F.; Ulgena, K. O. Bubble Column Reactors. *Process Biochem.* **2005**, *40*, 2263.

(17) Jager, B.; Espinoza, R. Advances in Low Temperature Fischer−Tropsch Synthesis. *Catal. Today* **1995**, *23*, 17.

(18) Gandhi, B.; Prakash, A.; Bergougnou, M. A. Hydrodynamic Behavior of Slurry Bubble Column at High Solids Concentrations. *Powder Technol.* **1999**, *103*, 80.

(19) Behkish, A.; Men, Z.; Inga, J. R.; Morsi, B. I. Mass Transfer Characteristics in a Large-Scale Slurry Bubble Column with Organic Liquid Mixtures. *Chem. Eng. Sci.* **2002**, *57*, 3307.

(20) Dry, M. E. Practical and Theoretical Aspects of the Catalytic Fischer−Tropsch Process. *Appl. Catal. A: Gen.* **1996**, *138*, 319.

(21) Wender, I. Reactions of Synthesis Gas. *Fuel Process. Technol.* **1996**, *48*, 189.

(22) de Swart, J. W. A.; Krishna, R.; Sie, S. T. Selection, Design and Scale-up of the Fischer−Tropsch Reactor. *Stud. Surf. Sci. Catal.* **1997**, *107*, 213.

(23) Lee, S. G.; Sardesai, A. Liquid Phase Methanol and Dimethyl Ether Synthesis from Syngas. *Top. Catal.* **2005**, *32*, 197.

(24) Sherwin, M. B.; Frank, M. C. Make Methanol by Three Phase Reaction. *Hydrocarbon Process.* **1976**, *55*, 122.

(25) Cybulski, A. Liquid-Phase Methanol Synthesis: Catalysts, Mechanism, Kinetics, Chemical Equilibria, Vapor-Liquid Equilibria, and Modeling − a Review. *Catal. Rev.* **1994**, *36*, 557.

(26) Yang, G. Q. ; Luo, X. ; Lau, R. ; Fan, L. S. Heat Transfer Characteristics in Slurry Bubble Columns at Elevated Pressures and Temperatures. *Ind. Eng. Chem. Res.* **2000**, *39*, 2568.

(27) Li, H.; Prakash, A.; Margaritis, A.; Bergougnou, M. A. Effects of Micron-Sized Particles on Hydrodynamics and Local Heat Transfer in a Slurry Bubble Column. *Powder Technol.* **2003**, *133*, 171.

(28) Lee, S.; Gogate, M. R.; Kulik, C. J. Novel Single-Step Dimethyl Ether (DME) Synthesis in a Three-Phase Slurry Reactor from CO-Rich Syngas. *Chem. Eng. Sci.* **1992**, *47*, 3769.

(29) Wang, Z. L.; Wang, J. F.; Diao, J.; Jin, Y. The Synergy Effect of Process Coupling for Dimethyl Ether Synthesis in Slurry Reactors. *Chem. Eng. Technol.* **2001**, *24*, 507.

(30) Sie, S. T.; Krishna, R. Fundamentals and Selection of Advanced Fischer−Tropsch Reactors. *Appl. Catal. A: Gen.* **1999**, *186*, 55.

(31) Dudukoviċ, M. P.; Larachi, F.; Mills, P. L. Multiphase Catalytic Reactors: a Perspective on Current Knowledge and Future Trends. *Catal. Rev.* **2002**, *44*, 123.

(32) Jin, Y.; Wang, T. F.; Wang, J. F.; Zhang, T. W. An Internal for Multiphase Reactors to Improve the Hydrodynamic and Transfer Behaviors. CN Patent 1,199,722C, 2003.

(33) Šetinc, M.; Levec, J. On the Kinetics of Liquid-Phase Methanol Synthesis over Commercial $Cu/ZnO/Al_2O_3$ Catalyst. *Chem. Eng. Sci.* **1999**, *54*, 3577.

(34) Van der Laan, G. P.; Beenackers, A. A. C. M. Kinetics and Selectivity of the Fischer−Tropsch Synthesis: A Literature Review. *Catal. Rev.* **1999**, *41*, 255.

(35) Raje, A. P.; Davis, B. H. Fischer−Tropsch Synthesis over Iron-Based Catalysts in a Slurry Reactor. Reaction Rates, Selectivities and Implications for Improving Hydrocarbon Productivity. *Catal. Today* **1997**, *36*, 335.

(36) Satterfield, C. N.; Huff, G. A., Jr. Effects of Mass Transfer on Fischer-Tropsch Synthesis in Slurry Reactors. *Chem. Eng. Sci.* **1980**, *35*, 195.

(37) Deckwer, W. D.; Serpemen, Y.; Ralek, M.; Schmidt, B. On the Relevance of Mass Transfer Limitations in the Fischer−Tropsch Slurry Process. *Chem. Eng. Sci.* **1981**, *36*, 765.

(38) Inga, J. R.; Morsi, B. I. A Novel Approach for the Assessment of the Rate-Limiting Step in Fischer−Tropsch Slurry Process. *Energy Fuel* **1996**, *10*, 566.

(39) Hyndman, C. L.; Larachi, F.; Guy, C. Understanding Gas-Phase Hydrodynamics in Bubble Columns: a Convective Model based on Kinetic Theory. *Chem. Eng. Sci.* **1997**, *52*, 63.

(40) Zahradník, J.; Fialová, M. The Effect of Bubbling Regime on Gas and Liquid Phase Mixing in Bubble Column Reactors. *Chem. Eng. Sci.* **1996**, *51*, 2491.

(41) Zuber, N.; Findlay, J. A. Average Volumetric Concentration in Two−Phase Flow Systems. *J. Heat Transfer* **1965**, *87*, 453.

(42) Vial, C.; Poncina, S.; Wild, G.; Midoux, N. Experimental and Theoretical Analysis of the Hydrodynamics in the Riser of an External Loop Airlift Reactor. *Chem. Eng. Sci.* **2002**, *57*, 4745.

(43) Drahoš, J.; Zahradník, J.; Puncochar, M.; Fialova, M.; Bradka, F. Effect of Operating Conditions of the Characteristics of Pressure Fluctuations in a Bubble Column. *Chem. Eng. Process.* **1991**, *29*, 107.

(44) Zhang, J. P.; Grace, J. R.; Epstein, N.; Lim, K. S. Flow Regime Identification in Gas-Liquid Flow and Three−Phase Fluidized Beds. *Chem. Eng. Sci.* **1997**, *52*, 3979.

(45) Maucci, E.; Briens, C. L.; Martinuzzi, R. J.; Wild, G. Detection and Characterization of Piston Flow Regime in Three−Phase Fluidized Beds. *Powder Technol.* **1999**, *103*, 243.

(46) Letzel, H. M.; Schouten, J. C.; Krishna, R.; van den Bleek, C. M. Characterization of Regimes and Regime Transitions in Bubble Columns by Chaos Analysis of Pressure Signals. *Chem. Eng. Sci*. **1997**, *52*, 4447.

(47) Thorat, B. N.; Joshi, J. B. Regime Transition in Bubble Columns: Experimental and Predictions. *Exp. Therm. Fluid Sci.* **2004**, *28*, 423.

(48) Wang, T. F.; Wang, J. F.; Jin, Y. Theoretical Prediction of Flow Regime Transition in Bubble Columns by the Population Balance Model. *Chem. Eng. Sci.* **2005**, *60*, 6199.

(49) Camarasa, E.; Vial, C.; Poncin, S.; Wild, G.; Midoux, N.; Bouillard, J. Influence of Coalescence Behaviour of the Liquid and of Gas Sparging on Hydrodynamics and Bubble Characteristics in a Bubble Column. *Chem. Eng. Process*. **1999**, *38*, 329.

(50) Ruzicka, M. C.; Drahoš, J.; Fialová, M.; Thomas, N. H. Effect of Bubble Column Dimensions on Flow Regime Transition. *Chem. Eng. Sci.* **2001**, *56*, 6117.

(51) Sriram, K.; Mann, R.. Dynamic Gas Disengagement: a New Technique for Assessing the Behaviour of Bubble Columns. *Chem. Eng. Sci.* **1977**, *32*, 571.

(52) Krishna, R.; De Stewart, J. W. A.; Ellenberger, J.; Martina, G. B.; Maretto, C. Gas Holdup in Slurry Bubble Columns: Effect of Column Diameter and Slurry Concentrations. *AIChE J.* **1997**, *43*, 311.

(53) Li, H.; Prakash, A. Influence of Slurry Concentrations on Bubble Population and Their Rise Velocities in Three−Phase Slurry Bubble Column. *Powder Technol.* **2000**, *113*, 158.

(54) Bakshi, B. R.; Zhong, H.; Jiang, P.; Fan, L. S. Analysis of Flow in Gas−Liquid Bubble Columns using Multi−Resolution methods. *Chem. Eng. Res. Des. Trans. Inst. Chem. Eng., Part A* **1995**, *73*, 608.

(55) Vial, C.; Camarasa, E.; Poncin, S.; Wild, G.; Midoux, N.; Bouillard, J. Study of Hydrodynamic Behaviour in Bubble Columns and External Loop Airlift Reactors Through Analysis of Pressure Fluctuations. *Chem. Eng. Sci.* **2000**, *55*, 2957.

(56) Lin, T. J.; Juang, R. C.; Chen, Y. C.; Chen, C. C. Prediction of Flow Transition in a Bubble Column by Chaotic Time Series Analysis of Pressure Fluctuation Signal. *Chem. Eng. Sci.* **2001**, *56*, 1057.

(57) Olmos, E.; Gentric, C.; Vial, C.; Wild, G.; Midoux, N. Numerical Simulation of Multiphase Flow in Bubble Column Reactors: Influence of Bubble Coalescence and Breakup. *Chem. Eng. Sci.* **2001**, *56*, 6359.

(58) Luo, H.; Svendsen, H. F. Modeling and Simulation of Binary Approach by Energy Conservation Analysis. *Chem. Eng. Commun.* **1996**, *145*, 145−153.

(59) Luo, H.; Svendsen, H. F. Theoretical Model for Drop and Bubble Breakup in Turbulent Dispersions. *AIChE J.* **1996**, *42*, 1225.

(60) Prince, M. J.; Blanch, H. W. Bubble Coalescence and Break-up in Air-Sparged Bubble Columns. *AIChE J.* **1990**, *36*, 1485.

(61) Hagesaether, L.; Jakobsen, H. A.; Svendsen, H. F. A Model for Turbulent Binary Breakup of Dispersed Fluid Particles. *Chem. Eng. Sci.* **2002**, *57*, 3251.

(62) Wang, T. F.; Wang, J. F.; Jin, Y. Novel Theoretical Breakup Kernel Function of Bubbles/Droplets in a Turbulent Flow. *Chem. Eng. Sci.* **2003**, *58*, 4629.

(63) Wang, T. F.; Wang, J. F.; Jin, Y. Population Balance Model for Gas−Liquid Flows: Influence of Bubble Coalescence and Breakup Models. *Ind. Eng. Chem. Res.* **2005**, *44*, 7540.

(64) Boyer, C.; Duquenne, A. M.; Wild, G. Measuring Techniques in Gas−Liquid and Gas−Liquid−Solid reactors. *Chem. Eng. Sci.* **2002**, *57*, 3185.

(65) Utiger, M.; Stuber, F.; Duquenne, A.; Delmas, H.; Guy, C. Local Measurements for the Study of External Loop Airlift Hydrodynamics. *Can. J. Chem. Eng.* **1999**, *77*, 375.

(66) Dziallas, H.; Michele, V.; Hempel, D. C. Measurement of Local Phase Holdups in a Two- and Three-Phase Bubble Column. *Chem. Eng. Technol.* **2000**, *23*, 877.

(67) Degaleesan, S.; Dudukovic, M.; Pan, Y. Experimental Study of Gas-Induced Liquid-Flow Structures in Bubble Columns. *AIChE J.* **2001**, *47*, 1913.

(68) Lin, J.; Han, M. H.; Wang, T. F.; Zhang, T. W.; Wang, J. F.; Jin, Y. Experimental Study on the Local Hydrodynamic Behavior of a Three-Phase External Loop Airlift Reactor. *Ind. Eng. Chem. Res.* **2004**, *43*, 5432.

(69) Wang, T. F.; Wang, J. F.; Zhao, B.; Ren, F.; Jin, Y. Local Hydrodynamics in External Loop Airlift Slurry Reactors with and without Resistance-Regulating Element. *Chem. Eng. Commun.* **2004**, *191*, 1024.

(70) de Swart, J. W. A.; van Vliet, R. E.; Krishna, R. Size, Structure, and Dynamics of "Large" Bubbles in a Two-Dimensional Slurry Bubble Column. *Chem. Eng. Sci.* **1996**, *51*, 4619.

(71) Lin, T. J.; Tsuchiya, K.; Fan, L. S. Bubble Flow Characteristics in Bubble Columns at Elevated Pressure and Temperature. *AIChE J.* **1998**, *44*, 545.

(72) Luo, X. K.; Lee, D. J.; Lau, R.; Yang, G. Q.; Fan, L. S. Maximum Stable Bubble Size and Gas Holdup in High−Pressure Slurry Bubble Columns. *AIChE J.* **1999**, *45*, 665.

(73) Lehr, F.; Millies, M.; Mewes, D. Bubble-Size Distributions and Flow Fields in Bubble Columns. *AIChE J.* **2002**, *48*, 2426.

(74) Wang, T. F.; Wang, J. F.; Jin, Y. A CFD−PBM Coupled Model for Gas−Liquid Flows. *AIChE J.* **2006**, *52*, 125.

(75) Chen, P.; Sanyal, J.; Dudukovic, M. P. Numerical Simulation of Bubble Columns Flows: Effect of Different Breakup and Coalescence Closures. *Chem. Eng. Sci.* **2005**, *60*, 1085.

(76) Fukuma, M.; Muroyama, K.; Morooka, S. Properties of Bubble Swarm in a Slurry Bubble Column. *J. Chem. Eng. Jpn.* **1987**, *20*, 28.

(77) Saxena, S. C.; Rao, N. S.; Saxena, A. C. Heat-Transfer and Gas-Holdup Studies in a Bubble Column: Air−Water−Glass Bead System. *Chem. Eng. Commun.* **1990**, *96*, 31.

(78) Akita, K.; Yoshida, F. Bubble size, interfacial area, and liquid phase mass transfer coefficients in bubble columns. *Ind. Eng. Chem., Process Des. Dev.* **1974**, *13*, 84−91.

(79) Wang, T. F.; Wang, J. F.; Yang, W. G.; Jin, Y. Bubble Behavior in Gas−Liquid−Solid Three-Phase Circulating Fluidized Beds. *Chem. Eng. J.* **2001**, *84*, 397.

(80) Vandu, C. O.; Koop, K.; Krishna, R. Large Bubble Sizes and Rise Velocities in a Bubble Column Slurry Reactor. *Chem. Eng. Technol.* **2004**, *27*, 1195.

(81) Schumpe, A.; Grund, G. The Gas Disengagement Technique for Studying Gas Holdup Structure in Bubble Columns. *Can. J. Chem. Eng.* **1986**, *64*, 891.

(82) Chen, R. C.; Reese, J.; Fan, L. S. Flow Structure in a Three-Dimensional Bubble Column and Three-Phase Fluidized Bed. *AIChE J.* **1994**, *40*, 1093.

(83) Zahradník, J.; Fialová, M.; Růžička, M.; Drahoš, J.; Kaštánek, F.; Thomas, N. H. Duality of the Gas−Liquid Flow Regimes in Bubble Column Reactors. *Chem. Eng. Sci.* **1997**, *52*, 3811.

(84) Wang, T. F.; Wang, J. F.; Jin, Y. Experimental Study and CFD Simulation of Hydrodynamic Behaviors in an External Loop Airlift Slurry Reactor. *Can. J. Chem. Eng.* **2004**, *82*, 1183.

(85) Shaikh, A.; Al-Dahhan, M. Characterization of the Hydrodynamic Flow Regime in Bubble Columns via Computed Tomography. *Flow Meas. Instrum.* **2005**, *16*, 91.

(86) Hibiki, T.; Ishii, M. Two-Group Interfacial Area Transport Equations at Bubbly-to-Slug Transition. *Nucl. Eng. Des.* **2000**, *202*, 39.

(87) Krishna, R.; Wilkinson, P. M.; Van Dierendonck, L. L. A Model for Gas Holdup in Bubble Columns Incorporating the Influence of Gas Density on Flow Regime Transitions. *Chem. Eng. Sci.* **1991**, *46*, 2491.

(88) Krishna, R.; Urseanu, M. I.; van Baten, J. M.; Ellenberger, J. Influence of Scale on the Hydrodynamics of Bubble Columns Operating in the Churn-Turbulent: Experiments vs. Eulerian Simulations. *Chem. Eng. Sci.* **1999**, *54*, 4903.

(89) Hills, J. H. Radial Non-Uniformity of Velocity and Voidage in a Bubble Column. *Trans. Inst. Chem. Eng.* **1974**, *52*, 1.

(90) Ohnuki, A.; Akimoto, H. Experimental Study on Transition of Flow Pattern and Phase Distribution in upward Air−Water Two-Phase Flow along a Large Vertical Pipe. *Int. J. Multiphase Flow* **2000**, *26*, 367.

(91) Kemoun, A.; Ong, B. C.; Gupta, P.; Al-Dahhan, M. H.; Dudukovic, M. P. Gas Holdup in Bubble Columns at Elevated Pressure via Computed Tomography. *Int. J. Multiphase Flow* **2001**, *27*, 929.

(92) Tomiyama, A.; Tamai, H.; Shimomura, H.; Hosokawa, S. Spatial Evolution of Developing Air−Water Bubble Flow in a Vertical Pipe. *Proc. Int. Symp. Two-Phase Flow Model. Exp.* **1999**, *2*, 1027; Pisa, Italy.

(93) Lucas, D.; Krepper, E.; Prasser, H. M. Prediction of Radial Gas Profiles in Vertical Pipe Flow on the Basis of Bubble Size Distribution. *Int. J. Therm. Sci.* **2001**, *40*, 217.

(94) Lin, J.; Han, M. H.; Wang, T. F.; Zhang, T. W.; Wang, J. F.; Jin, Y. Influence of the Gas Distributor on the Local Hydrodynamic Behavior of an External Loop Airlift Reactor. *Chem. Eng. J.* **2004**, *102*, 51.

(95) Wu, Y. X.; Al-Dahhan, M. H. Prediction of Axial Liquid Velocity Profile in Bubble Columns. *Chem. Eng. Sci.* **2001**, *56*, 1127.

(96) Menzel, T.; Weide, T.; Staudacher, O.; Wein, O.; Onken, U. Reynolds Shear Stress for Modeling of Bubble Reactors. *Ind. Eng. Chem. Res.* **1990**, *29*, 988.

(97) Luo, H.; Svendsen, H. F. Turbulent Circulation in Bubble Columns from Eddy Viscosity Distributions of Single-Phase Pipe Flow. *Can. J. Chem. Eng.* **1991**, *69*, 1389.

(98) Zehner, P. Momentum, Mass and Heat Transfer in Bubble Columns, Part 1 Flow Model of the Bubble Column and Liquid Velocities. *Int. Chem. Eng.* **1986**, *26*, 22.

(99) Riquarts, H. P. A Physical Model for Axial Mixing of the Liquid Phase for Heterogeneous Flow Regime in Bubble Columns. *Ger. Chem. Eng.* **1981**, *4*, 18.

(100) Krishna, R.; van Baten, J. M.; Urseanu, M. I. Three-Phase Eulerian Simulations of Bubble Column Reactors Operating in the Churn-Turbulent Regime: a Scale up Strategy. *Chem. Eng. Sci.* **2000**, *55*, 3275.

(101) Li, H.; Prakash, A. Heat Transfer and Hydrodynamics in a Three-Phase Slurry Bubble Column. *Ind. Eng. Chem. Res.* **1997**, *36*, 4688.

(102) Urseanu, M. I.; Guit, R. P. M.; Stankiewicz, A.; van Kranenburg, G.; Lommen, J. H. G. M. Influence of Operating Pressure on the Gas Hold-up in Bubble Columns for High Viscous Media. *Chem. Eng. Sci.* **2003**, *58*, 697.

(103) Kuncová, G.; Zahradník, J. Gas Holdup and Bubble Frequency in a Bubble Column Reactor Containing Viscous Saccharose Solutions. *Chem. Eng. Process.* **1995**, *34*, 25.

(104) Kozo, K.; Seiji, Y.; Shigehiko, H. Effects of Surface-Active Substances on Gas Holdup and Gas-Liquid Mass Transfer in Bubble Column. *J. Chem. Eng. Jpn*. **1985**, *18*, 287.

(105) Zahradník, J.; Kuncová, G.; Fialová, M. The Effect of Surface Active Additives on Bubble Coalescence and Gas Holdup in Viscous Aerated Batches. *Chem. Eng. Sci.* **1999**, *54*, 2401.

(106) Dargar, P.; Macchi, A. Effect of Surface-Active Agents on the Phase Holdups of Three-Phase Fluidized Beds. *Chem. Eng. Process.* **2006**, *45*, 764.

(107) Hikita, H.; Asal, S.; Tanigawa, K.; Segawa, K.; Kitao, M. Gas Holdup in Bubble Column. *Chem. Eng. J.* **1980**, *20*, 59.

(108) Sada, E.; Katoh, S.; Yoshil, H. Performance of the Gas−Liquid Bubble Column in Molten Salt Systems. *Ind. Eng. Chem., Process Des. Dev.* **1984**, *23*, 151.

(109) Veera, U. P.; Kataria, K. L.; Joshi, J. B. Gas Hold-up Profiles in Foaming Liquids in Bubble Columns. *Chem. Eng. J.* **2001**, *84*, 247.

(110) Veera, U. P.; Kataria, K. L.; Joshi, J. B. Effect of Superficial Gas Velocity on Gas Hold-up Profiles in Foaming Liquids in Bubble Column Reactors. *Chem. Eng. J.* **2004**, *99*, 53.

(111) Fan, L. S.; Yang, G. Q.; Lee, D. J.; Tsuchiya1, K.; Luo, X. Some Aspects of High-Pressure Phenomena of Bubbles in Liquids and Liquid−Solid Suspensions. *Chem. Eng. Sci.* **1999**, *54*, 4681.

(112) Fan, L. S.; Tsuchiya, K. *Bubble Wake Dynamics in Liquids and Liquid-Solid Suspensions*; Butterworth-Heinemann: Stoneham, MA, 1990.

(113) Oyevaar, M. H.; De La Rie, T.; Van Der Sluijs, C. L.; Westerterp, K. R. Interfacial Areas and Gas Hold-ups in Bubble Columns and Packed Bubble Columns at Elevated Pressures. *Chem. Eng. Process.* **1989**, *26*, 1.

(114) Wilkinson, P. M.; van Dierendonck, L. L. Pressure and Gas Density Effects on Bubble Break-up and Gas Hold-up in Bubble Columns. *Chem. Eng. Sci.* **1990**, *45*, 2309.

(115) Lemoine, R.; Behkish, A.; Morsi, B. I. Hydrodynamic and Mass-Transfer Characteristics in Organic Liquid Mixtures in a Large-Scale Bubble Column Reactor for the Toluene Oxidation Process. *Ind. Eng. Chem. Res.* **2004**, *43*, 6195.

(116) Reilly, I. G.; Scott, D. S.; De Bruijn, T. J. W.; MacIntyre, D. Role of Gas Phase Momentum is Determining Gas Holdup and Hydrodynamic Flow Regimes in Bubble Column Operations. *Can. J. Chem. Eng.* **1994**, *72*, 3.

(117) Letzel, H. M.; Schouten, J. C.; Krishna, R.; van den Bleek, C. M. Gas Holdup and Mass Transfer in Bubble Column Reactors Operated at Elevated Pressure. *Chem. Eng. Sci.* **1999**, *54*, 2237.

(118) Kang, Y.; Cho, Y. J.; Woo, K. J.; Kim, S. D. Diagnosis of Bubble Distribution and Mass Transfer in Pressurized Bubble Columns with Viscous Liquid Medium. *Chem. Eng. Sci.* **1999**, *54*, 4887.

(119) Jordan, U.; Schumpe, A. The Gas Density Effect on Mass Transfer in Bubble Columns with Organic Liquids. *Chem. Eng. Sci.* **2001**, *56*, 6267.

(120) Deckwer, W. D.; Louisi, Y.; Zaidi, A.; Ralek, M. Hydrodynamic Properties of the Fischer−Tropsch Slurry Process. *Ind. Eng. Chem., Process Des. Dev.* **1980**, *19*, 699.

(121) Vandu, C. O.; Koop, K.; Krishna, R. Volumetric Mass Transfer Coefficient in a Slurry Bubble Column Operating in the Heterogeneous Flow Regime. *Chem. Eng. Sci.* **2004**, *59*, 5417.

(122) Jiang, P.; Lin, T. J.; Luo, X.; Fan, L. S. Flow Visualization of High Pressure (21 MPa) Bubble Column: Bubble Characteristics. *Chem. Eng. Res. Des. Trans. Inst. Chem. Eng., Part A* **1997**, *75*, 269.

(123) Letzel, M. H. Effect of Gas Density on Large-Bubble Holdup in Bubble Column Reactors. *AIChE J.* **1998**, *44*, 2333.

(124) Sagert, N. H.; Quinn, M. J. Coalescence of H_2S and CO_2 Bubbles in Water. *Can. J. Chem. Eng.* **1976**, *54*, 392.

(125) Lanauze, R. D.; Harris, I. J. A Note on Gas Bubble Formation Models. *Chem. Eng. Sci.* **1974**, *29*, 1663.

(126) Soong, Y.; Harke, F. W.; Gamwo, I. K.; Schehl, R. R.; Zarochak, M. F. Hydrodynamic Study in a Slurry-Bubble-Column Reactor. *Catal. Today* **1997**, *35*, 427.

(127) Pohorecki, R.; Moniuk, W.; Zdrojkowski, A.; Bielski, P. Hydrodynamics of a Pilot Plant Bubble Column under Elevated Temperature and Pressure. *Chem. Eng. Sci.* **2001**, *56*, 1167.

(128) Schäfer, R.; Merten, C.; Eigenberger, G. Bubble Size Distributions in a Bubble Column Reactor under Industrial Conditions. *Exp. Therm. Fluid Sci.* **2002**, *26*, 595.

(129) Lau, R.; Peng, W.; Velazquez−Vargas, L. G.; Yang, G. Q.; Fan, L. S. Gas−Liquid Mass Transfer in High-Pressure Bubble Columns. *Ind. Eng. Chem. Res.* **2004**, *43*, 1302.

(130) Vandu, C. O.; Krishna, R. Volumetric Mass Transfer Coefficient in Slurry Bubble Columns Operating in the Churn-Turbulent Flow Regime. *Chem. Eng. Process.* **2004**, *43*, 987.

(131) Mooney, M. The Viscosity of a Concentrated Suspension of Spherical Particles. *J. Colloid Sci.* **1951**, *6*, 162.

(132) Simha, R. A Treatment of the Viscosity of Concentrated Suspensions. *J. Appl. Phys.* **1952**, *23*, 1020.

(133) Thomas, G. D. Transport Characteristics of Suspension: VIII. A Note on the Viscosity of Newtonian Suspensions of Uniform Spherical Particles. *J. Colloid Sci.* **1965**, *20*, 267.

(134) Leighton, D.; Acrivos, A. Viscous Resuspension. *Chem. Eng. Sci.* **1986**, *41*, 1377.

(135) Tsuchiya, K.; Furumoto, A.; Fan, L. S.; Zhang, J. P. Suspension Viscosity and Bubble Rise Velocity in Liquid−Solid Fluidized Beds. *Chem. Eng. Sci.* **1997**, *52*, 3053.

(136) Brady, J. F. Computer Simulation of Viscous Suspensions. *Chem. Eng. Sci.* **2001**, *56*, 2921.

(137) Usui, H. Prediction of Dispersion Characteristics and Rheology in Dense Slurries. *J. Chem. Eng. Jpn.* **2002**, *35*, 815.

(138) Perez, M.; Barbe, J. C.; Neda, Z.; Brechet, Y.; Salvo, L. Computer Simulation of the Microstructure and Rheology of Semi−Solid Alloys under Shear. *Acta Mater.* **2000**, *48*, 3773.

(139) Zhao, R.; Goodwin, J. G.; Oukaci, R. Attrition Assessment for Slurry Bubble Column Reactor Catalysts. *Appl. Catal. A: Gen.* **1999**, *189*, 99.

(140) Luo, X. K.; Zhang, J. P.; Tsuchiya, K.; Fan, L. S. On the Rise Velocity of Bubbles in Liquid−Solid Suspensions at Elevated Pressure and Temperature. *Chem. Eng. Sci.* **1997**, *52*, 3693.

(141) Prakash, A.; Margaritis, A.; Li, H. Hydrodynamics and Local Heat Transfer Measurements in a Bubble Column with Suspension of Yeast. *Biochem. Eng. J.* **2001**, *9*, 155.

(142) Inga, J. R.; Morsi, B. I. Effect of Operating Variables on the Gas Holdup in a Large-Scale Slurry Bubble Column Reactor Operating with an Organic Liquid Mixture. *Ind. Eng. Chem. Res.* **1999**, *38*, 928.

(143) Kara, S.; Kelkar, B. G.; Shah, Y. T.; Carr, N. L. Hydrodynamics and Axial Mixing in a Three-Phase Bubble Column. *Ind. Eng. Chem., Process. Des. Dev.* **1982**, *21*, 584.

(144) Kato, Y.; Nishiwaki, A.; Kago, T.; Fukuda, T.; Tanaka, S. Gas Holdup and Overall Volumetric Absorption Coefficient in Bubble Columns with Suspended Solid Particles. *Int. Chem. Eng.* **1973**, *13*, 562.

(145) Boer, A.; Schrauwen, F. J. M. Gas Distributor for a Reactor. Patent WO 2005/084790, 2005.

(146) Coppens, M. O. Method for Operating a Chemical and/or Physical Process by Means of a Hierarchical Fluid Injection System. Patent WO 00/66257, 2000.

(147) Bouaifi, M.; Hebrard, G.; Bastoul, D.; Roustan, M. A Comparative Study of Gas Holdup, Bubble Size, Interfacial Area and Mass Transfer Coefficients in Stirred Gas−Liquid Reactors and Bubble Columns. *Chem. Eng. Process.* **2001**, *40*, 97.

(148) Espinoza, R. L.; Steynberg, A. P.; Harding, S.; Labuschagne, J. Hydrogenation of Hydrocarbons. Patent WO 98/37168, 1998.

(149) Shah, Y. T.; Kelkar, B. G.; Godbole, S. P. Design Parameters Estimations for Bubble Column Reactors. *AIChE J.* **1982**, *28*, 353.

(150) Wilkinson, P. M.; Spek, A. P.; van Dierendonck, L. L. Design Parameters Estimation for Scale-up of High-Pressure Bubble Columns. *AIChE J.* **1992**, *38*, 544.

(151) Yamashita, F. Effect of Liquid Depth, Column Inclination and Baffle Plates on Gas Holdup in Bubble Columns. *J. Chem. Eng. Jpn.* **1985**, *18*, 349.

(152) Kumar, S. B.; Moslemian, D.; Dudukovic, M. P. Gas-Holdup Measurements in Bubble Columns Using Computed Tomography. *AIChE J.* **1997**, *43*, 1414.

(153) Thorat, B. N.; Shevade, A. V.; Bhilegaonkar, K. N.; Aglawe, R. H.; Veera, U. P.; Thakre, S. S.; Pandit, A. B.; Sawant, S. B.; Joshi, J. B. Effect of Sparger Design and Height to Diameter Ratio on Fractional Gas Hold-up in Bubble Columns. *Chem. Eng. Res. Des. Trans. Inst. Chem. Eng., Part A* **1998**, *76*, 823.

(154) Veera, U. P.; Joshi, J. B. Measurement of Gas Hold-up Profiles by Gamma Ray Tomography: Effect of Sparger Design and Height of Dispersion in Bubble Column. *Chem. Eng. Res. Des. Trans. Inst. Chem. Eng., Part A* **1999**, *77*, 303.

(155) Deckwer, W. D.; Schumpe, A. Improved Tools for Bubble Column Reactor Design and Scale-up. *Chem. Eng. Sci.* **1993**, *48*, 889.

(156) Maruyama, T.; Yoshida, S.; Mizushina, T. Flow Transition in a Bubble Column. *J. Chem. Eng. Jpn.* **1981**, *14*, 352.

(157) Sarrafi, A.; Jamialahmadi, M.; Muller−Steinhagen, H.; Smith, J. M. Gas Holdup in Homogeneous and Heterogeneous Gas−Liquid Bubble Column Reactors. *Can. J. Chem. Eng.* **1999**, *77*, 11.

(158) Zhu, J. W.; Trivedi, V. H.; Saxena, S. C. Gas-Phase Holdup in a Slurry-Bubble Column. *Chem. Eng. Commun.* **1997**, *157*, 53.

(159) Yamashita, F. Gas Holdup in Bubble Column with Draft Tube for Gas Dispersion into Annulus. *J. Chem. Eng. Jpn.* **1998**, *31*, 289.

(160) Forret, A.; Schweitzer, J. M.; Gauthier, T.; Krishna, R.; Schweich, D. Influence of Scale on the Hydrodynamics of Bubble Column Reactors: an Experimental Study in Columns of 0.1, 0.4 and 1 m Diameters. *Chem. Eng. Sci.* **2003**, *58*, 719.

(161) Wijffels, R. H.; Verheul, M.; Beverloo, W. A.; Tramper, J. Liquid/Solid Mass Transfer in an Air-Lift Loop Reactor with a Dispersed Solid Phase. *J. Chem. Technol. Biotechnol.* **1998**, *71*, 147.

(162) Maalej, S.; Benaddam, B.; Otterbein, M. Interfacial Area and Volumetric Mass Transfer Coefficient in a Bubble Reactor at Elevated Pressures. *Chem. Eng. Sci.* **2003**, *58*, 2365.

(163) Elgozali, A.; Linek, V.; Fialova, M.; Wein, O.; Zahradnik, J. Influence of Viscosity and Surface Tension on Performance of Gas−Liquid Contactors with Ejector Type Gas Distributor. *Chem. Eng. Sci.* **2002**, *57*, 2987.

(164) Chaumat, H.; Billet-Duquenne, A. M.; Augier, F.; Mathieu, C.; Delmas, H. Mass Transfer in Bubble Column for Industrial Conditions − Effects of Organic Medium, Gas and Liquid Flow Rates and Column Design. *Chem. Eng. Sci.* **2005**, *60*, 5930.

(165) Yang, W. G.; Wang, J. F.; Zhou, L. M.; Jin, Y. Gas-Liquid Mass Transfer Behavior in Three-Phase CFB Reactors. *Chem. Eng. Sci.* **1999**, *54*, 5523.

(166) Yang, W. G.; Wang, J. F.; Wang, T. F.; Jin, Y. Experimental Study on Gas−Liquid Interfacial Area and Mass Transfer Coefficient in Three-Phase Circulating Fluidized Beds. *Chem. Eng. J.* **2001**, *84*, 485.

(167) Tang, W. T.; Fan, L. S. Hydrodynamics of a Three-Phase Fluidized Bed Containing Low-Density Particles. *AIChE J.* **1989**, *35*, 355.

(168) Wilkinson, P. M.; Haringa, H.; van Dierendonck, L. L. Mass Transfer and Bubble Size in a Bubble Column under Pressure. *Chem. Eng. Sci.* **1994**, *49*, 1417.

(169) Kojima, H.; Sawai, J.; Suzuki, H. Effect of Pressure on Volumetric Mass Transfer Coefficient and Gas Holdup in Bubble Column. *Chem. Eng. Sci.* **1997**, *52*, 4111.

(170) Yang, W. G.; Wang, J. F.; Jin, Y. Mass Transfer Characteristics of Syngas Components in Slurry System at Industrial Conditions. *Chem. Eng. Technol.* **2001**, *24*, 651.

(171) Jin, H. B.; Liu, D. L.; Yang, S. H.; He, G. X.; Guo, Z. W.; Tong, Z. M. Experimental Study of Oxygen Mass Transfer Coefficient in Bubble Column with High Temperature and High Pressure. *Chem. Eng. Technol.* **2004**, *27*, 1267.

(172) Ozturk, S. S.; Schumpe, A.; Deckwer, W. D. Organic Liquids in a Bubble Column: Holdups and Mass Transfer Coefficients. *AIChE J.* **1987**, *33*, 1473.

(173) Dewes, I.; Schumpe, A. Gas Density Effect on Mass Transfer in the Slurry Bubble Column. *Chem. Eng. Sci.* **1997**, *52*, 4105.

(174) Koide, K.; Takazawa, A.; Komura, M.; Matsunga, H. Gas Holdup and Volumetric Liquid Phase Mass Transfer Coefficient in Solid-Suspended Bubble Column. *J. Chem. Eng. Jpn.* **1984**, *17*, 459.

(175) Okada, K.; Nagata, Y.; Akagi, Y. Effect of Packed Bed on Mass Transfer in External-Loop Airlift Bubble Column. *J. Chem. Eng. Jpn.* **1996**, *29*, 582.

(176) Bai, F.; Wang, L.; Huang, H.; Xu, J.; Caesar, J.; Ridgway, D.; Gu, T.; Moo-Young, M. Oxygen Mass-Transfer Performance of Low Viscosity Gas−Liquid−Solid System in a Split-Cylinder Airlift Bioreactor. *Biotechnol. Lett.* **2001**, *23*, 1109.

(177) Quicker, G.; Schumpe, A.; Deckwer, W. D. Gas−Liquid Interfacial Areas in a Bubble Column with Suspended Solids. *Chem. Eng. Sci.* **1984**, *39*, 179.

(178) Smith, B. C.; Skidmore, D. R. Mass Transfer Phenomena in an Airlift Reactor. Effect of Solids Loading and Temperature. *Biotechnol. Bioeng.* **1990**, *35*, 483.

(179) Feitkenhauer, H.; Maleski, R.; Markl, H. Airlift-Reactor Design and Test for Aerobic Environmental Bioprocesses with Extremely High Solid Contents at High Temperature. *Water Sci. Technol.* **2003**, *48*, 69.

(180) Muller, F. L.; Davidson, F. On the Effects of Surfactants on Mass Transfer to Viscous Liquids in Bubble Columns. *Chem. Eng. Res. Des.* **1995**, *73*, 291.

(181) Vasconcelos, J. M. T.; Rodrigues, J. M. L.; Orvalho, S. C. P.; Alves, S. S.; Mendes, R. L.; Reis, A. Effect of Contaminants on Mass Transfer Coefficients in Bubble Column and Airlift Contactors. *Chem. Eng. Sci.* **2003**, *58*, 1431.

(182) Vázquez, G.; Cancela, M. A.; Riverol, C.; Alvarez, E.; Navaza, J. M. Application of the Danckwerts Method in a Bubble Column: Effects of Surfactants on Mass Transfer Coefficient and Interfacial Area. *Chem. Eng. J.* **2000**, *78*, 13.

(183) Painmanakul, P.; Loubièrea, K.; Hébrard, G.; Mietton-Peuchot, M.; Roustan, M. Effect of Surfactants on Liquid-Side Mass Transfer Coefficients. *Chem. Eng. Sci.* **2005**, *60*, 6480.

(184) Azher, N. E.; Gourich, B.; Vial, C.; Bellhaj, M. S.; Bouzidi, A.; Barkaoui, M.; Ziyad, M. Influence of Alcohol Addition on Gas Hold-up, Liquid Circulation Velocity and Mass Transfer Coefficient in a Split-Rectangular Airlift Bioreactor. *Biochem. Eng. J.* **2005**, *23*, 161.

(185) Sardeing, R.; Painmanakul, P.; Hébrard, G. Effect of Surfactants on Liquid-Side Mass Transfer Coefficients in Gas−Liquid Systems: A First Step to Modeling. *Chem. Eng. Sci.* **2006**, *61*, 6249.

(186) Stegeman, D.; Knop, P. A.; Wijnands, A. J. G.; Westerterp, K. R. Interfacial Area and Gas Holdup in a Bubble Column Reactor at Elevated Pressures. *Ind. Eng. Chem. Res.* **1996**, *35*, 3842.

(187) Pohorecki, R.; Moniuk, W.; Zdrojkowski, A. Hydrodynamics of a Bubble Column under Elevated Pressure. *Chem. Eng. Sci.* **1999**, *54*, 5187.

(188) Srinivasan, R.; Xu, L.; Spicer, R. L.; Tungate, F. L.; Davis, B. H. Fischer−Tropsch Catalysts. Attrition of Carbided Iron Catalyst in the Slurry Phase. *Fuel Sci. Technol. Int.* **1996**, *14*, 1337.

(189) Zhou, P. Z.; Srivastava, R. D. *Status Review of Fischer−Tropsch Slurry Reactor Catalyst/Wax Separation Techniques*; Prepared for the U.S. Department of Energy, Pittsburgh Energy Technology Center: Pittsburgh, PA, 1991.

(190) Benham, C. B.; Yakobson, D. L.; Bohn, M. S. Catalyst/Wax Separation Device for Slurry Fischer−Tropsch Reactor. US Patent 6,068,-760, 2000.

(191) Clerici, G. C. E.; Belmonte, G. Separation/Filtration Device used in a Process for the Production of Hydrocarbons from Synthesis Gas in Slurry Reactors. GB Patent 2,403,433, 2005.

(192) Rytter, E.; Lian, P.; Myrstad, T.; Roterud, P.T.; Solbakken, A. Method of Conducting Catalytic Converter Multi-Phase Reaction. US Patent 5,422,375, 1993.

(193) Jager, B.; Steynberg, A. P.; Inga, J. R.; Kellkens, R. C.; Smith, M. A.; Malherbe, F. E. J. Process for Producing Liquid and, Optionally, Gaseous Products from Gaseous Reactants. US Patent 5,599,849, 1997.

(194) Anderson, J. H. Internal Filter for Fischer−Tropsch Catalyst/Wax Separation. US Patent 6,652,760, 2003.

(195) Müller, P. Guaranteeing Process Industries High Product Quality & Yield. *Filtr. Sep.* **2003**, *40*, 34.

(196) White, C. M.; Quiring, M. S.; Jensen, K. L.; Hickey, R. F.; Gillham, L. D. Separation of Catalyst from Fischer−Tropsch Slurry. US Patent 5,827,903, 1998.

(197) Brioles, J. M.; Wan, Y. D.; Kilpatric, P. K.; Roberts, G. W. Separation of Fischer−Tropsch Wax from Catalyst using Near-Critical Fluid Extraction: Analysis of Process Feasibility. *Energy Fuel* **1999**, *13*, 667.

(198) Brennan, J. A.; Chester, A. W. ; Chu, Y. F.; High Gradient Magnetic Separation. US Patent 4,605,678, 1986.

(199) Espinoza, R. L.; Mohedas, S. R.; Odueyungbo, S.; Ortego, J. D. Solid−Liquid Separation System. US Patent 6,833,078, 2004.

(200) Bello, R. A.; Robinson, C. W.; Moo-Young, M. Prediction of the Volumetric Mass Transfer Coefficient in Pneumatic Contactor. *Chem. Eng. Sci.* **1985**, *40*, 53.

(201) Weiland, P.; Onken, U. Differences in the Behaviour of Bubble Columns and Airlift Loop Reactors. *Ger. Chem. Eng.* **1981**, *4*, 174.

(202) Kawase, Y.; Hashiguchi, N. Gas−Liquid Mass Transfer in External-Loop Airlift Columns with Newtonian and non-Newtonian Fluids. *Chem. Eng. J.* **1996**, *62*, 35.

(203) Lu, W. J.; Hwang, S. J.; Chang, C. M. Liquid Velocity and Gas Holdup in Three-Phase Internal Airlift Reactors with Low-Density Particles. *Chem. Eng. Sci.* **1995**, *50*, 1301.

(204) Freitas, C.; Fialová, M.; Zahradnik, J.; Teixeira, J. A. Hydrodynamics of a Three-Phase External-Loop Airlift Bioreactor. *Chem. Eng. Sci.* **2000**, *55*, 4961.

(205) Hwang, S. J.; Cheng, Y. L. Gas Holdup and Liquid Velocity in Three-Phase Internal-Loop Airlift Reactors. *Chem. Eng. Sci.* **1997**, *52*, 3949.

(206) García-Calvo, E.; Rodríguez, A.; Prados, A.; Klein, J. A Fluid Dynamic Model for Three-Phase Airlift Reactors. *Chem. Eng. Sci.* **1999**, *54*, 2359.

(207) Couvert, A.; Roustan, M.; Chatellier, P. Two-Phase Hydrodynamic Study of a Rectangular Air-Lift Loop Reactor with an Internal Baffle. *Chem. Eng. Sci.* **1999**, *54*, 5245.

(208) Dreher, A. J.; Krishna, R. Liquid-Phase Backmixing in Bubble columns, Structured by Introduction of Partition Plates. *Catal. Today* **2001**, *69*, 165.

(209) Bando, Y.; Fujimori, K.; Terazawa, H.; Yasuda, K.; Nakamura, M. Effects of Equipment Dimensions on Circulation Flow Rates of Liquid and Gas in Bubble Column with Draft Tube. *J. Chem. Eng. Jpn.* **2000**, *33*, 379.

(210) Chisti, Y.; Kasper, M.; Moo-Young, M. Mass Transfer in External−Loop Airlift Bioreactors using Static Mixers. *Can. J. Chem. Eng.* **1990**, *68*, 45.

(211) Lin, C. H.; Fang, B. S.; Wu, C. S.; Fang, H. Y.; Kuo, T. F.; Hu, C. Y. Oxygen Transfer and Mixing in a Tower Cycling Fermentor. *Biotechnol. Bioeng.* **1976**, *18*, 1557−1572.

(212) Stejskal, J.; Potucek, F. Oxygen Transfer in Liquids. *Biotechnol. Bioeng.* **1985**, *27*, 503.

(213) Nikakhtari, H.; Hill, G. A. Enhanced Oxygen Mass Transfer in an External Loop Airlift Bioreactor using a Packed Bed. *Ind. Eng. Chem. Res.* **2004**, *43*, 6195.

(214) Bendjaballah, N.; Dhaouadi, H.; Poncin, S.; Midoux, N.; Hornut, J. M.; Wild, G. Hydrodynamics and Flow Regimes in External Loop Airlift Reactors. *Chem. Eng. Sci.* **1999**, *54*, 5211.

(215) Krichnavaruk, S.; Pavasant, P. Analysis of Gas−Liquid Mass Transfer in an Airlift Contactor with Perforated Plate. *Chem. Eng. J.* **2002**, *89*, 203.

(216) Zhang, T. W.; Wang, J. F.; Wang, T. F.; Lin, J.; Jin, Y. Effect of Internal on the Hydrodynamics in External-Loop Airlift Reactors. *Chem. Eng. Process.* **2005**, *44*, 81.

(217) Yu, W.; Wang, T. F.; Liu, M. L.; Wang, Z. W. Study on the Hydrodynamics in a Multi-Stage Internal-Loop Airlift Slurry Reactor. *The 9th China−Japan Symposium on Fluidization*, Beijing, China, December 18−20, 2006; 155.

(218) Xia, Y. K.; Peng, F. F.; Wolfe, E. CFD Simulation of Alleviation of Fluid Back Mixing by Baffles in Bubble Column. *Miner. Eng.* **2006**, *19*, 925.

(219) Alvaréa, J.; Al-Dahhanb, M. H. Liquid Phase Mixing in Trayed Bubble Column Reactors. *Chem. Eng. Sci.* **2006**, *61*, 1819.

(220) Oey, R. S.; Mudde, R. F.; Portela, L. M.; van den Akker, H. E. A. Simulation of a Slurry Airlift using a Two-Fluid Model. *Chem. Eng. Sci.* **2001**, *56*, 673.

(221) Delnoij, E.; Lammers, F. A.; Kuipers, J. A. M.; Van Swaaij, W. P. M. Dynamic Simulation of Dispersed Gas−Liquid Two-Phase Flow using a Discrete Bubble Model. *Chem. Eng. Sci.* **1997**, *52*, 1429.

(222) Sokolichin, A.; Eigenberger, G.; Lapin, A.; Lübbert, A. Dynamic Numerical Simulation of Gas−Liquid Two-Phase Flows: Euler−Euler versus Euler−Lagrange. *Chem. Eng. Sci.* **1997**, *52*, 611.

(223) Drew, D. A. Mathematical Modeling of Two-Phase Flow. *Annu. Rev. Fluid Mech.* **1983**, *15*, 261.

(224) Lahey, R. T.; Drew, D. A. On the Development of Multidimensional Two-Fluid Models for Vapor/Liquid Two-Phase Flows. *Chem. Eng. Commun.* **1992**, *118*, 125.

(225) Jakobsen, H. A.; Sannes, B. H.; Grevskott, S.; Svendsen, F. Modeling of Vertical Bubble-Driven Flows. *Ind. Eng. Chem. Res.* **1997**, *36*, 4052.

(226) Jakobsen, H. A.; Lindborg, H.; Dorao, C. A. Modeling of Bubble Column Reactors: Progress and Limitations. *Ind. Eng. Chem. Res.* **2005**, *44*, 5107.

(227) Rafique, M.; Chen, P.; Dudukovic, M. P. Computational Modeling of Gas−Liquid Flow in Bubble Columns. *Rev. Chem. Eng.* **2004**, *20*, 225.

(228) Jakobsen, H. A. Phase Distribution Phenomena in Two-Phase Bubble Column Reactors. *Chem. Eng. Sci.* **2001**, *56*, 1049.

(229) Pan, Y.; Dudukovic, M. P.; Chang, M. Dynamic Simulation of Bubbly Flow in Bubble Columns. *Chem. Eng. Sci.* **1999**, *54*, 2481.

(230) Hua, J.; Wang, C. H. Numerical Simulation of Bubble-Driven Liquid Flows. *Chem. Eng. Sci.* **2000**, *55*, 4159.

(231) Pfleger, D.; Becker, S. Modelling and Simulation of the Dynamic Flow Behaviour in a Bubble Column. *Chem. Eng. Sci.* **2001**, *56*, 1737.

(232) Colella, D.; Vinci, D.; Bagatin, R.; Masi, M.; Bakr, E. A. A Study on Coalescence and Breakage Mechanisms in Three Different Bubble Columns. *Chem. Eng. Sci.* **1999**, *54*, 4767.

(233) Sha, Z.; Laari, A.; Turunen, I. Implementation of Population Balance into Multiphase-Model in CFD Simulation for Bubble Column. *CHISA 16th International Congress of Chemical Process Engineering*, Prague, Czech Republic, August 22−26, 2004; 445.

(234) Liu, T. J.; Bankoff, S. G. Structure of Air−Water Bubbly Flow in a Vertical Pipe−II. Void Fraction, Bubble Velocity and Bubble Size Distribution. *Int. J. Heat Mass Transfer* **1993**, *36*, 1061.

Received for review March 3, 2007
Revised manuscript received May 17, 2007
Accepted June 13, 2007

IE070330T